

COUNTING COLOURED BOXES

by

Benjamin Young

B.Sc., Carleton University, 2001

M.Sc., Carleton University, 2002

A THESIS SUBMITTED IN PARTIAL FULFILMENT OF
THE REQUIREMENTS FOR THE DEGREE OF

Doctor of Philosophy

in

THE FACULTY OF GRADUATE STUDIES

(Mathematics)

THE UNIVERSITY OF BRITISH COLUMBIA

(Vancouver)

April 2008

© Benjamin Young 2008

Abstract

This thesis consists of the manuscripts of two research papers. In the first paper, we verify a recent conjecture of Kenyon/Szendrői by computing the generating function for pyramid partitions. Pyramid partitions are closely related to Aztec Diamonds; their generating function turns out to be the partition function for the Donaldson–Thomas theory of a non-commutative resolution of the conifold singularity $\{x_1x_2 - x_3x_4 = 0\} \subset \mathbb{C}^4$. The proof does not require algebraic geometry; it uses a modified version of the domino (or dimer) shuffling algorithm of Elkies, Kuperberg, Larsen and Propp.

In the second paper, we derive two multivariate generating functions for three-dimensional Young diagrams (also called plane partitions). The variables correspond to a colouring of the boxes according to a finite abelian subgroup G of $SO(3)$. These generating functions turn out to be orbifold Donaldson–Thomas partition functions for the orbifold $[\mathbb{C}^3/G]$. We need only the vertex operator methods of Okounkov–Reshetikhin–Vafa for the easy case $G = \mathbb{Z}_n$; to handle the considerably more difficult case $G = \mathbb{Z}_2 \times \mathbb{Z}_2$, we will also use a refinement of the author’s recent q -enumeration of pyramid partitions.

In the appendix, written by Jim Bryan, we relate the diagram generating functions to the Donaldson–Thomas partition functions of the orbifold $[\mathbb{C}^3/G]$. We find a relationship between the Donaldson–Thomas partition functions of the orbifold

and its G -Hilbert scheme resolution. We formulate a crepant resolution conjecture for the Donaldson-Thomas theory of local orbifolds satisfying the Hard Lefschetz condition.

Contents

Abstract	ii
Contents	iv
List of figures	vii
Acknowledgements	ix
Dedication	x
Co-authorship statement	xi
1 Introduction	1
1.1 Introduction	2
1.2 Thesis theme and objectives	3
1.3 Literature review	3
Bibliography	5
2 Counting pyramid partitions with dimer shuffling	6
2.1 Introduction	7
2.2 Dimer shuffling	12
2.3 Weighting the lattice	16

2.4	Weighting and shuffling	20
2.5	Length- ∞ pyramid partitions	23
2.6	A weight-preserving bijection	27
2.7	The generating function for general n	31
2.8	Conclusion	32
	Bibliography	34
3	Counting 3D Young diagrams with vertex operators	35
3.1	Introduction	36
3.2	Review: the infinite wedge space	42
3.3	The operators $\Gamma(x)$, $\Gamma'(x)$, and Q_g	45
3.4	Counting with \mathbb{Z}_n colouring	48
3.5	Pyramid partitions	52
3.6	A generating function for pyramid partitions	60
3.7	Counting $\mathbb{Z}_2 \times \mathbb{Z}_2$ -coloured 3D Young diagrams	62
3.8	Future work	67
	Bibliography	69
4	Conclusion	71
4.1	Directions for future research	72
4.2	Relevance of the research	72
4.3	Strengths and weaknesses of the research	73
	Bibliography	74
A	Donaldson-Thomas theory of \mathbb{C}^3/G and its crepant resolution (by Dr. Jim Bryan)	75
A.1	Review of Donaldson-Thomas theory	76

A.2	Orbifold Donaldson-Thomas theory of $[\mathbb{C}^3/G]$	77
A.3	The Donaldson-Thomas crepant resolution conjecture	84
A.3.1	Proof of Proposition A.3.2 / Theorem 3.1.7:	87
	Bibliography	89

List of Figures

2.1	Special bricks, assembled into the configuration ε_3 .	7
2.2	A pyramid partition of length 1	9
2.3	The empty rooms of lengths 1 and 2.	9
2.4	Odd blocks, even blocks, and shuffling directions	13
2.5	The sliding map	14
2.6	Elementary moves for adding a bricks to pyramid partitions	17
2.7	The w_0 weighting on the square lattice	19
2.8	A comparison of the weightings w_0 and w_1	21
2.9	A pyramid partition being split into two pieces	24
2.10	The weighting w_∞ , top and bottom pieces.	25
2.11	The empty room of length ∞ , ε_∞ , top and bottom halves	26
2.12	Elementary moves for generating elements of \mathcal{P}_∞ from ε_∞	27
2.13	A super-rigid partition is a pyramid partition of length ∞	29
3.1	A partition coloured according to $K_{\mathbb{Z}_2 \times \mathbb{Z}_2}$ and to $K_{\mathbb{Z}_3}$	40
3.2	Applying α_{-3} to a partition	44
3.3	Slicing a \mathbb{Z}_3 -coloured 3D diagram	50
3.4	A pyramid partition, removed from the pyramid	52
3.5	A quiver diagram for colouring pyramid partitions	54

3.6	A view of the pyramid \mathcal{B} from below	55
3.7	A diagonal slice of a pyramid partition is a 2D Young diagram . .	57
3.8	The j th columns of two adjacent slices π_0, π_1	59
3.9	Row- and column-interlacing behaviour in a pyramid partition . .	59
3.10	Slicing a $\mathbb{Z}_2 \times \mathbb{Z}_2$ -coloured 3D diagram	63

Acknowledgements

The author would like to thank Jim Bryan and Richard Kenyon for their help, good advice, and many fruitful discussions. In addition, the author would like to thank Dr. Balázs Szendrői for introducing the problem of enumerating pyramid partitions.

Dedication

I would like to dedicate this thesis to my wife Rachael and to my parents Meralin and Joe Young.

Co-authorship statement

Identification and design of research program

The research program for Chapter 2 was entirely mine. My advisor, Jim Bryan, introduced me to the counting problems in Chapter 3, and conjectured the statement of Theorem 3.1.5. The remainder of the research planning (choosing combinatorial techniques to try, and looking for related work done by others) were done by me.

Research and data analysis

The research for Chapter 2 was entirely mine. In Chapter 3, Jim Bryan did the portion of the work which relates the enumerative results to Donaldson–Thomas theory. The remainder of the work is mine. The research did not involve any data analysis, except for early computer investigations which I conducted.

Manuscript preparation

I wrote and typeset Chapter 2 completely. I wrote and typeset all of Chapter 3 with the exception of the portions of the introduction having to do with Donaldson–Thomas theory, which were written by Jim Bryan and typeset by me. Jim Bryan also wrote the appendix on Donaldson–Thomas Theory.

Chapter 1

Introduction

1.1 Introduction

This thesis answers several variants of the following problem: How many different ways are there to stably stack n boxes in the corner of a room? These stable stacks of boxes are called *three-dimensional Young diagrams*, or sometimes *3D partitions* or *plane partitions* elsewhere in the literature.

The modern way to answer this question is by giving a *generating function*: we write down a formal power series in q such that the coefficient of q^n is the answer that we seek. The answer to this simplest version of the problem is

$$\sum_{\pi \text{ 3D partition}} q^{|\pi|} = \prod_{n=1}^{\infty} \left(\frac{1}{1 - q^n} \right)^n, \quad (1.1)$$

as computed by MacMahon [5]. The problems considered in this thesis involve two variations on this theme:

- We consider different shaped stacks of boxes, called *pyramid partitions*, as well as 3D Young diagrams.
- We give multivariate generating functions in variables q_g , where g runs over some finite group G , some index set. The boxes in the diagrams are assigned different colours in a prescribed pattern which respects the multiplication rule of G , and the coefficients of the generating function allow one to determine how many ways to stack the boxes given a certain number of boxes of each colour if one follows the pattern.

1.2 Thesis theme and objectives

The overall theme of the thesis is, obviously, to count piles of colored boxes; however, there is an underlying theme of exploring the relationships between pyramid partitions and 3D Young diagrams. On the one hand, Chapter 2 uses a technique called *dimer shuffling* to reduce the question of enumerating pyramid partitions to a well-known computation in Donaldson–Thomas theory: a certain weighted count of 3D Young diagrams which share a common asymptotic leg of boxes. On the other hand, Chapter 3 uses the calculus of vertex operators to evaluate certain coloured generating functions on 3D Young diagrams and on pyramid partitions; the pyramid partition result is in turn applied to count 3D Young diagrams coloured according to the action of the group $\mathbb{Z}_2 \times \mathbb{Z}_2$. It is likely that such links are symptomatic of a deeper connection between these types of objects, but so far we do not know what that connection might be.

1.3 Literature review

The question of enumerating pyramid partitions was raised in [8, 4], and the theorems of Chapter 2 were conjectured there based on computational evidence. Pyramid partitions arose implicitly in [7] as the height functions of dimer covers on the square lattice.

There is an extensive literature on 3D Young diagrams, beginning with MacMahon’s work [5]. Many other proofs of (1.1) are known – see the introduction to Chapter 3. Very little has been published on “coloured” enumerating problems, with the exception of [3, 1]; these papers prove a generating function which can be easily specialized to count 3D Young diagrams with \mathbb{Z}_n colouring. The result

on $\mathbb{Z}_2 \times \mathbb{Z}_2$ -colouring is new.

The dimer shuffling technique used in Chapter 2 were pioneered in [2] for the purpose of counting Aztec Diamonds. The vertex operator machinery used in Chapter 3 was first used to count 3D Young diagrams by Okounkov [7] and Okounkov–Reshetikhin [6].

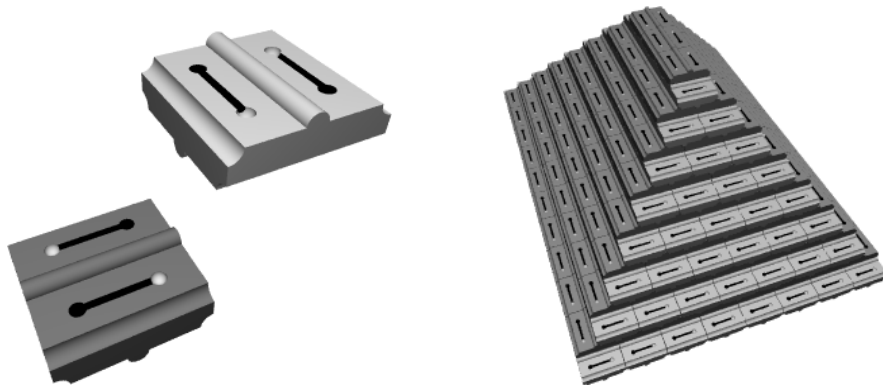
Bibliography

- [1] George G. Andrews and Peter Paule. MacMahon's dream. Preprint, <http://www.math.psu.edu/andrews/preprints.html>.
- [2] Noam Elkies, Greg Kuperberg, Michael Larsen, and James Propp. Alternating sign matrices and domino tilings ii. *Journal of Algebraic Combinatorics*, 1(3):219–234, November 1992.
- [3] Emden R. Gansner. The enumeration of plane partitions via the Burge correspondence. *Illinois J. Math*, 25(2):533–554, 1981.
- [4] Richard Kenyon. Talk at the workshop on random partitions and Calabi-Yau crystals, Amsterdam, 2005. Available at <http://www.math.brown.edu/~rkenyon/talks/pyramids.pdf>.
- [5] Percy A. MacMahon. *Combinatory Analysis*. Cambridge University Press, The Edinburgh Building, Cambridge, UK, 1915-16.
- [6] Andrei Okounkov and Nikolai Reshetikhin. Correlation function of Schur process with application to local geometry of a random 3-dimensional Young diagram. *J. Amer. Math. Soc.*, 16(3):581–603, 2003.
- [7] Andrei Okounkov, Nikolai Reshetikhin, and Cumrun Vafa. Quantum Calabi-Yau and classical crystals. *Progress in Mathematics*, 244:597–618, November 2006.
- [8] Balázs Szendrői. Non-commutative Donaldson-Thomas theory and the conifold. To appear in *Geometry and Topology*. arXiv:0705.3419v1 [math.AG].

Chapter 2

Counting pyramid partitions with dimer shuffling

Figure 2.1: Special bricks, assembled into the configuration ε_3 .



2.1 Introduction

Consider the pyramid-shaped stack of square bricks shown in Figure 2.1 . The bricks are the same ones used to q -enumerate Aztec Diamonds in [2]: ridges on the top and bottom of the bricks restrict the manner in which the bricks may be stacked. Each brick rests upon two side-by-side bricks, and is rotated 90 degrees from the bricks immediately below it. We use two colors of bricks – light and dark – to make alternating layers of this pyramid, starting with dark bricks at the pyramid’s apex.

In Figure 2.1, there is a row of three dark bricks at the top of the pyramid. It is straightforward to build a similar pyramid with a row of $n \geq 1$ bricks along the top. Following [6], we make the following definitions:

Definition 2.1.1 *The pyramid with a row of n dark bricks at the top is called the*

⁰A version of this chapter has been submitted for publication. Young, B. Computing a pyramid partition generating function with dimer shuffling.

empty room¹ of length n , and is denoted ε_n .

Definition 2.1.2 A pyramid partition of length n is a finite subset π of the bricks of ε_n such that if B is a brick in π , then all of the bricks of ε_n which rest upon B are also in π . Let \mathcal{P}_n denote the set of all pyramid partitions of length n .

Definition 2.1.3 The weight of π , $w_0(\pi)$, is

$$q_0^{\#\{\text{dark bricks in } \pi\}} q_1^{\#\{\text{light bricks in } \pi\}}.$$

In other words, a pyramid partition is a collection of bricks removed from ε_n such that the remaining pile of bricks is stable. For our treatment, it is better to draw pyramid partitions by drawing the remaining pile of bricks. For an example of a pyramid partition drawn in this way, see Figure 2.2. Note that ε_n is itself a pyramid partition of weight 1, for all n .

There is a third way to view a pyramid partition π , which is much more useful computationally. Recall that a *dimer cover* (or *1-factor*) of a graph G is a subgraph G' such that every vertex of G' has degree 1. Each brick in π has two dimers stencilled on the top; dark bricks have vertical (North-South) dimers, whereas light bricks have horizontal (East-West) dimers. When one views π from above, one can see a dimer cover of the square lattice (see the right-hand image in Figure 2.2). It is helpful to think of the lattice points as pairs of half-integers, so that the origin lies above the axis of symmetry of ε_n .

Since every pyramid partition has only finitely many bricks, the dimer cover associated to π looks like that of ε_n (see Figure 2.3) when one moves far enough

¹This admittedly strange terminology is borrowed from the jargon of 3D partitions, which are made of stacks of boxes in the corner of a room. Here, the configuration of minimum weight is an empty room, with no boxes.

Figure 2.2: A pyramid partition of length 1, viewed from the side and from above

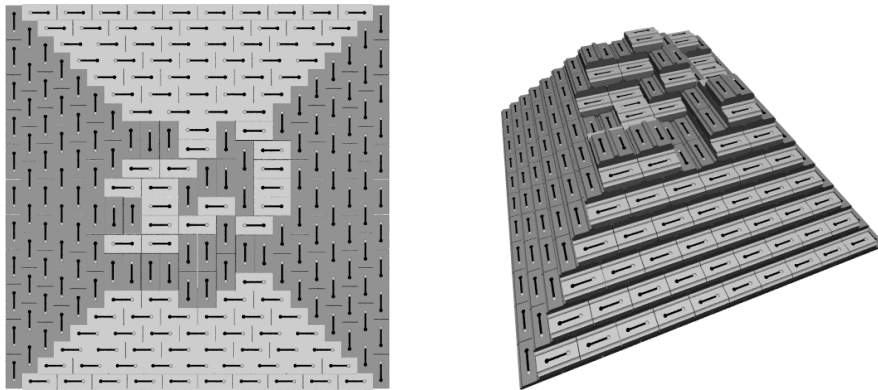
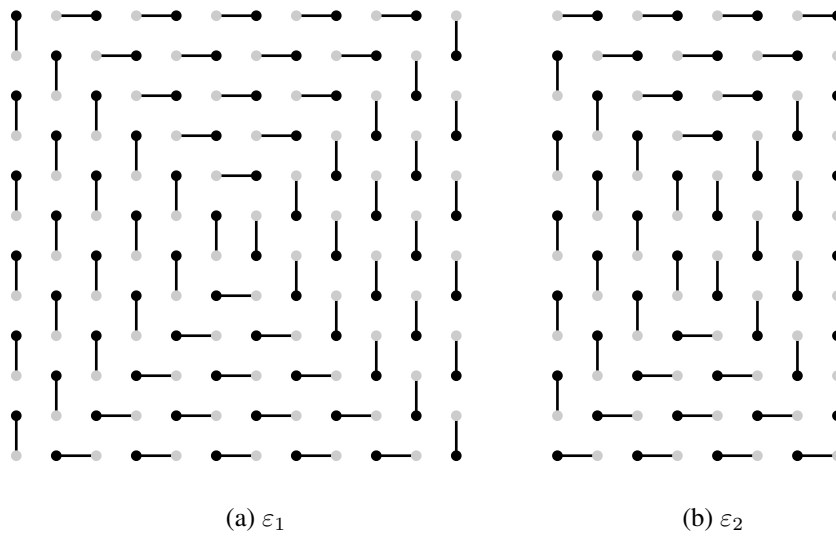


Figure 2.3: The empty rooms of lengths 1 and 2.



from the origin. Indeed, given a dimer cover T of the square lattice which is asymptotically identical to ε_n , it is straightforward to construct a corresponding pyramid partition which looks like T from above: the correspondence is bijective. We shall therefore refer to these dimer configurations as pyramid partitions, as well.

In [6], Szendrői defines a bivariate generating function for \mathcal{P}_n by

$$Z_A^{(n)}(q_0, -q_1) = \sum_{\pi \in \mathcal{P}_n} w_0(\pi)$$

and observes that $Z_A^{(1)}(q_0, q_1)$ arises as the partition function for the Donaldson–Thomas theory of a non-commutative resolution of the conifold singularity $\{x_1x_2 - x_3x_4 = 0\} \subset \mathbb{C}^4$. Szendrői conjectures that

$$Z_A^{(n)}(q_0, -q_1) = M(1, q_0q_1)^2 \prod_{k \geq 1} (1 + q_0^k q_1^{k-1})^{k+n-1} \prod_{k \geq 1} (1 + q_0^k q_1^{k+1})^{\max(k-n+1, 0)} \quad (2.1)$$

where $M(x, q)$ is the MacMahon function

$$M(x, q) = \prod_{n=1}^{\infty} \left(\frac{1}{1 - xq^n} \right)^n.$$

This conjecture (or at least the special case $q_0 = q_1 = q$) was originally posed by Kenyon [3].

We present a proof of this conjecture. We first do the case $n = 1$, using a modification of the domino shuffling argument of [2], originally used to compute the weight generating function of an Aztec Diamond. Strikingly, this case uses the Donaldson-Thomas partition function of the resolution of this conifold, computed in [1].

Before we go any further, let us choose a more convenient notation.

Definition 2.1.4 *Let*

$$Z(n; q_0, q_1) := Z_A^{(n)}(q_0, -q_1) = \sum_{\pi \in \mathcal{P}_n} w_0(\pi);$$

$$Z(\infty; q_0, q_1) := M(1, q_0 q_1)^2 M(-q_1^{-1}, q_0 q_1)^{-1}.$$

We may now restate (and prove) Equation (2.1) for $n = 1$ in the following form:

Theorem 2.1.5 $Z(1; q_0, q_1) = M(-q_1^{-1}, q_0 q_1)^{-1} Z(\infty; q_0, q_1).$

We have chosen the notion somewhat suggestively here. Our proof, *very* informally speaking, is that domino shuffling transforms pyramid partitions of length n into pyramid partitions of length $n + 1$ in a weight-preserving manner (the transformation is not quite bijective). Repeating this procedure forever, we get “pyramid partitions of length ∞ ”. These objects are easily weight-enumerated due to a surprising bijection with a type of $3D$ partitions which we have called *super-rigid partitions* (see Section 2.6). It is also possible to use our methods to prove equation (2.1) for general n , which in our new notation looks like this:

$$Z(n; q_0, q_1) = M(1, q_0 q_1)^2 \prod_{k \geq 1} (1 + q_0^k q_1^{k-1})^{k+n-1} \prod_{k \geq 1} (1 + q_0^k q_1^{k+1})^{\max(k-n+1, 0)} \quad (2.2)$$

In section 7, we shall outline how to modify our proof of Theorem 2.1.5 to handle this more general case. The proof is relegated to a later section of the chapter because it contains essentially no new combinatorial ideas (only greater complication) and $n = 1$ case is of greater geometric interest.

2.2 Dimer shuffling

Next, we will describe the shuffling algorithm, originally published in [2]. We shall call this algorithm *dimer shuffling*, rather than domino shuffling, since all of our pictures are of dimers, which are dual to the dominos of [2]. However, the shuffling algorithm is identical. We review it here in order to define all of our terminology.

The purpose of the algorithm is to transform a pyramid partition of length n into a pyramid partition of length $n + 1$. Unfortunately, the dimer shuffle is not quite an honest function from \mathcal{P}_n to \mathcal{P}_{n+1} ; one can only say that it sends a collection of pyramid partitions of length n to a related collection of length $n + 1$. So let us first describe the bijective part of the algorithm, the *sliding map*, which acts on certain partial dimer covers T of the square lattice.

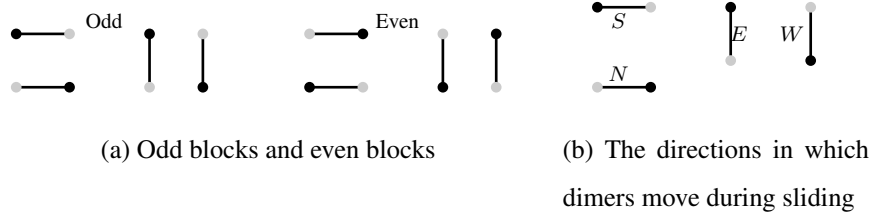
First of all, we colour the vertices of the lattice black and white in a checker-board pattern. Any dimer on this lattice has one endpoint of each color. Of course, we must pick the parity of this colouring; it depends on the parity of n (see Figure 2.3). If n is odd, then the center square of the lattice has a black vertex in the upper left corner. Otherwise, that vertex is white.

We adopt the following definitions of [2] (changing the notation slightly):

Definition 2.2.1 *Two side-by-side dimers (or, sometimes, their four endpoints) are called a block. A block is odd if it has a black vertex in the upper left corner; otherwise it is even.*

Figure 2.4(a) shows the different types of odd and even blocks. As you can see in Figure 2.3, the empty room of length n always has precisely n odd blocks in a vertical line in the center.

Figure 2.4



Definition 2.2.2 An odd-deficient (respectively, even-deficient) dimer cover is a partial dimer cover such that the set of non-covered vertices is a finite union of odd (respectively, even) blocks. Given a dimer cover T , construct the odd-deficient dimer cover \tilde{T} by deleting all of the odd blocks of T . Construct the even-deficient dimer cover \hat{T} by deleting all of the even blocks of T . Let

$$\tilde{\mathcal{P}}_n := \{\tilde{\pi} : \pi \in \mathcal{P}_n\},$$

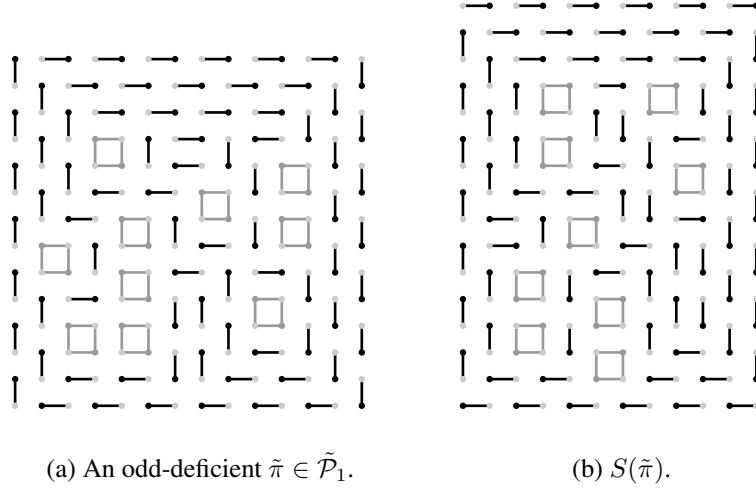
$$\hat{\mathcal{P}}_n := \{\hat{\pi} : \pi \in \mathcal{P}_n\}.$$

Definition 2.2.3 The sliding map S is a mapping from the set {dimers on the colored square lattice} to itself. If d is a dimer, then define $S(d)$ to be the other dimer in the odd block containing d . If T is an odd-deficient partial dimer cover, then define $S(T)$ to be the partial dimer cover $\{S(d) : d \in T\}$.

Observe that S moves each dimer in T one unit to the north, south, east, or west, depending on its position; Figure 2.4(b) shows the directions in which the dimers move. We shall often call dimers *northbound*, *southbound*, *eastbound*, or *westbound*, according to the direction in which they slide. Note that S depends on the parity of the lattice coloring we have chosen.

Lemma 2.2.4 S is an involution on the set of odd-deficient dimer covers. The restriction $S|_{\tilde{\mathcal{P}}_n}$ is a bijection from $\tilde{\mathcal{P}}_n$ to $\hat{\mathcal{P}}_{n+1}$ with their usual colorings.

Figure 2.5



Proof. One first shows that S is an involution, essentially by analyzing all of the possible local odd-deficient configurations of dimers. This is done in detail in [2]. To verify that the image of S is $\widehat{\mathcal{P}}_{n+1}$, observe that $S(\tilde{\varepsilon}_n) = \varepsilon_{n+1}$. The parity of the usual coloring of \mathcal{P}_{n+1} is the opposite of that of \mathcal{P}_n , so for $\pi \in \mathcal{P}_n$, $S(\pi)$ is even-deficient and asymptotic to ε_{n+1} . \square

Figure 2.5 shows how S works. In (a), we have deleted all of the odd blocks of the pyramid partition in Figure 2.2; the missing odd blocks are marked with grey squares. In (b), we have applied S , and now the grey squares denote the missing even blocks. Observe that $S(\pi) \in \widehat{\mathcal{P}}_2$.

We may now define the dimer shuffling algorithm, which extends S to a map

$$S : \mathcal{P}_n \rightarrow \{\text{formal sums of pyramid partitions of length } n+1\}.$$

Definition 2.2.5 *Let $\pi \in \mathcal{P}_n$. The following three steps constitute the dimer shuf-*

fling algorithm:

1. *(Deleting)* Delete all of the odd blocks in π to get $\tilde{\pi}$.
2. *(Sliding)* Compute $S(\tilde{\pi})$, as defined above.
3. *(Creating)* Now we have a partial dimer cover which is possibly missing some even blocks. Each block may be filled in with either two horizontal dimers, or two vertical dimers. Define $S(\pi)$ to be the formal sum of all of these fillings.

It is fairly straightforward to see that these steps are well-defined and that they do indeed give you a formal sum of dimer covers of the plane; this is shown in detail in [2].

Finally, let us prove a lemma about the number of odd blocks of a pyramid partition. Observe that Figure 2.5(a) has 10 odd blocks, whereas (b) has 9 even blocks. In general, we have:

Lemma 2.2.6 *Let $\tilde{\pi} \in \tilde{\mathcal{P}}_n$. Then $\#\{\text{odd blocks in } \tilde{\pi}\} - \#\{\text{even blocks in } S(\tilde{\pi})\} = n$.*

Proof. Suppose there are m odd blocks in π and m' even blocks in $S(\pi)$. Let R be a $2a \times (2a + 2n - 2)$ rectangle of lattice points centered at the origin, where a is large enough that π is identical to ε_n outside R , and there are no odd blocks of π on the boundary of R . For example, for the odd-deficient partition of Figure 2.5(a), we could take $a = 7$ and R to be the 14×14 rectangle of lattice points shown in the illustration.

Each dimer has two endpoints and each (missing) odd block has four vertices, so the number of dimers in R is

$$\frac{(2a)(2a + 2n - 2) - 4m}{2}. \quad (2.3)$$

Now let us shuffle the dimers in R . The same dimers now fit into a $(2a - 2) \times (2a + 2n)$ rectangle, which has $(2a - 2)(2a + 2n)$ lattice points, and contains all m' odd blocks. So the number of dimers in R is also equal to

$$\frac{(2a - 2)(2a + 2n) - 4m'}{2} \quad (2.4)$$

Setting Equations (2.3) and (2.4) equal, we obtain the lemma. \square

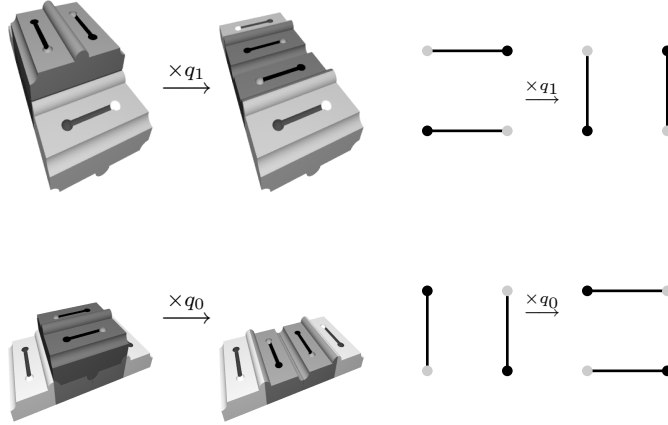
2.3 Weighting the lattice

In order to use domino shuffling as a computational tool, we need to find a way to calculate the weight of a pyramid partition from its dimer form, without interpreting it as a pile of bricks. Our strategy shall be to assign a monomial weight to every edge of the square lattice in such a way that the normalized product of the edge weights of any pyramid partition π is $w_0(\pi)$. This idea is mentioned in [6], but we shall need to be explicit about what edge weights we use and how we do the normalization.

In order to determine the proper weights to use, it is helpful to consider how a minimal change in the dimer configuration should affect the weight. We make the following definition:

Definition 2.3.1 *Let π be a pyramid partition. An elementary move is the act of adding an appropriately colored block to π to obtain a new pyramid partition.*

Figure 2.6: Elementary moves for adding a bricks to pyramid partitions



When we analyze the effect an elementary move has on the dimer version of π , we see that there are two different types of elementary moves for adding a dark or light brick. They are shown in Figure 2.6; recall that our convention in drawing the brick pictures is to show the *complement* of the pyramid partition! An odd elementary move should contribute q_0 to the weight, whereas an even move should contribute q_1 .

We may now assign a weight to each edge of the square lattice which is compatible with the elementary moves, in the following sense: select any 2×2 block of vertices in the weighted lattice. If it is an odd block, we should have

$$\frac{\text{weight of two horizontal dimers}}{\text{weight of two vertical dimers}} = q_0,$$

and if it is an even block, we should have

$$\frac{\text{weight of two vertical dimers}}{\text{weight of two horizontal dimers}} = q_1.$$

In fact, there are many ways to do this, but it is convenient to choose the

weighting in which all vertical edges have weight 1, and all the northbound horizontal edges closest to the x axis have weight 1 (see Figure 2.7). We adopt the convention that in a weighted lattice, edges with no marked weight get weight 1.

Definition 2.3.2 *If d is a dimer, then $w_0(d)$ is the weight assigned to d in Figure 2.7. Explicitly, $w_0(d) = 1$ if d is vertical; if d is horizontal, then*

$$w_0(d) = \begin{cases} (q_0 q_1)^{-t} & \text{if } d \text{ is centered at } (2s, 2t - \frac{1}{2}), s, t \in \mathbb{Z} \\ q_0 (q_0 q_1)^t & \text{if } d \text{ is centered at } (2s, 2t + \frac{1}{2}), s, t \in \mathbb{Z} \\ q_1^{-1} (q_0 q_1)^t & \text{if } d \text{ is centered at } (2s + 1, 2t - \frac{1}{2}), s, t \in \mathbb{Z} \\ (q_0 q_1)^{-t} & \text{if } d \text{ is centered at } (2s + 1, 2t + \frac{1}{2}), s, t \in \mathbb{Z} \end{cases}$$

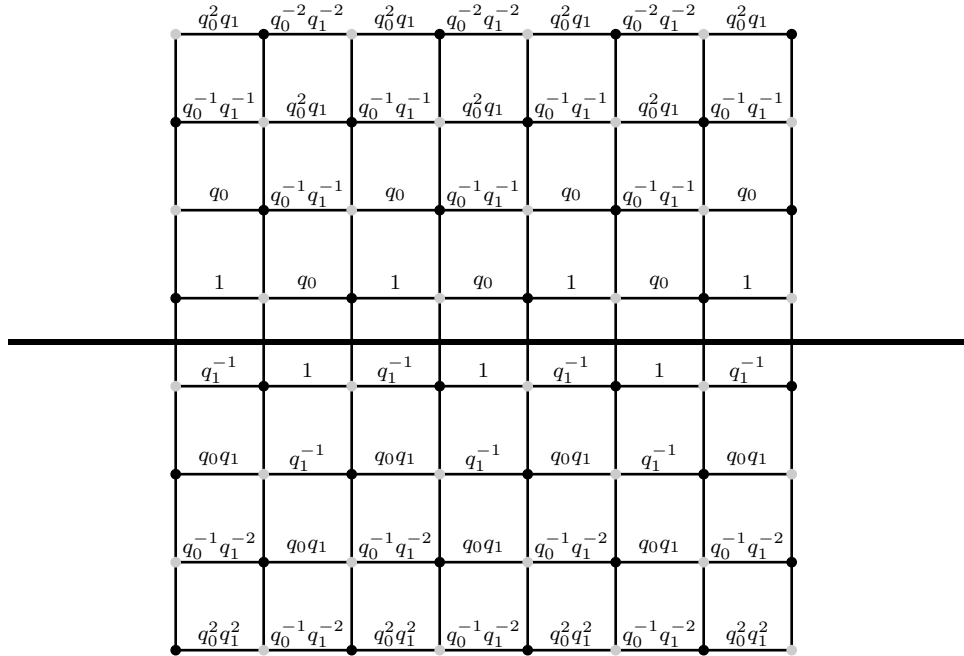
Now we need to explain how to use these edge weights to compute the weight of a pyramid partition π . Naively, we want to say that the weight of π is the product of the weights of its edges. However, since π covers the entire plane and has an infinite number of edges, this is meaningless. Fortunately, all one has to do is to normalize the weight in the following sense:

Lemma 2.3.3 *Suppose that $\pi \in \mathcal{P}_n$. Let R be a finite region of the lattice which contains all of the edges where π differs from ε_n . Then*

$$w_0(\pi) = \left(\prod_{e \in R \cap \pi} w_0(e) \right) \left(\prod_{e \in R \cap \varepsilon_n} w_0(e) \right)^{-1}.$$

Proof. As a base case, let $\pi = \varepsilon_n$ and observe that both sides are equal to 1. Next, suppose that the lemma holds for some pyramid partition π_0 ; by the preceding remarks, it also holds for all π which differ from π_0 by an elementary move. The lemma then follows by induction on the number of bricks in π . \square

Figure 2.7: The w_0 weighting on the square lattice. The heavy black line is the x axis.



2.4 Weighting and shuffling

We shall use a different weighting function, w_1 , to weight $S(\pi)$. Essentially, we want to think of the weight of a dimer as being unaffected by the shuffling operation. In fact, we shall define a series of weight functions w_1, w_2, w_3, \dots , which have the property that

$$w_0(d) = w_1(S(d)) = w_2(S^2(d)) = \dots$$

for any dimer d .

Definition 2.4.1 *Let d be dimer in a pyramid partition of length n (with the usual lattice coloring). Let $a \geq 1$. Define the weight function w_a by*

$$w_a(d) = w_0(\underbrace{S^{-1} \circ S^{-1} \circ \dots \circ S^{-1}}_{a-1}(d)).$$

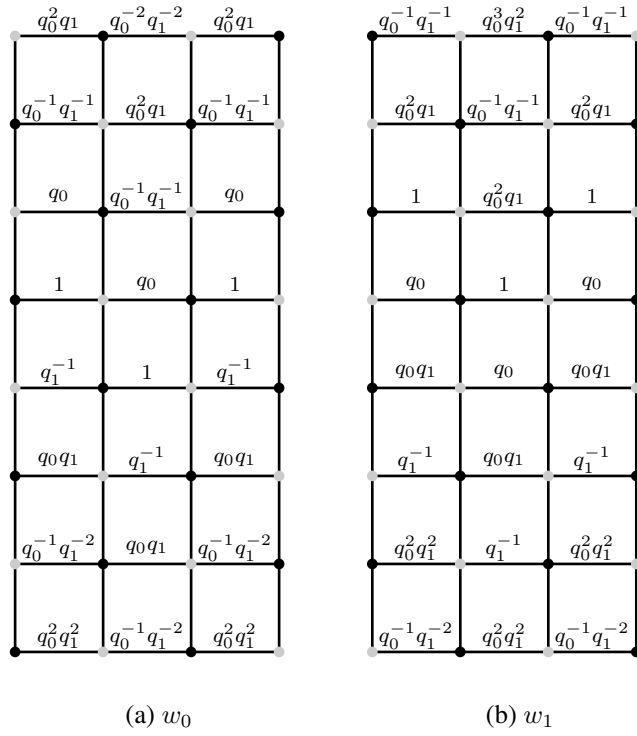
For a comparison of w_0 and w_1 , see Figure 2.8. Observe that if d is a vertical dimer, then $w_a(d) = 1$ for all a . In [2], there is only one weighting function, w_0 , and the generating function is manipulated so that w_0 can be reused.

Lemma 2.4.2 *Let d, d' be horizontal dimers, with d' immediately north of d . Then*

$$w_a(d)w_a(d') = \begin{cases} q_0^{a+1}q_1^a & \text{if the block formed by } d, d' \text{ is odd,} \\ q_0^aq_1^{a-1} & \text{if the block formed by } d, d' \text{ is even.} \end{cases}$$

Proof. When $a = 0$, the lemma follows from the definition of w_0 . Now, suppose $a > 0$. If the block d, d' is even, then S^{-1} interchanges d and d' , so

$$w_a(d)w_a(d') = w_{a-1}(S^{-1}(d))w_{a-1}(S^{-1}(d')) = w_{a-1}(d')w_{a-1}(d) = q_0^aq_1^{a-1}$$

Figure 2.8: A comparison of the weightings w_0 and w_1 

by induction on a ; otherwise, $(d, S^{-1}(d))$ and $(d', S^{-1}(d'))$ are odd blocks under the alternate coloring, and we have

$$\begin{aligned} w_a(d)w_a(d') &= w_{a-1}(S^{-1}(d))w_{a-1}(S^{-1}(d')) \\ &= \frac{w_{a-1}(S^{-1}(d))w_a(d)w_a(d')w_{a-1}(S^{-1}(d'))}{w_a(d)w_a(d')} \\ &= \frac{(q_0^a q_1^{a-1})^2}{q_0^{a-1} q_1^{a-2}} = q_0^{a+1} q_1^a \end{aligned}$$

again by induction on a . \square

Next, we define what we mean by the weight of an odd-deficient or even-deficient dimer cover:

Definition 2.4.3 *Let $\tilde{\eta}$ be an odd-deficient (or even-deficient) pyramid partition of length n . Let π be the pyramid partition obtained by filling in the missing odd (even) blocks of $\tilde{\eta}$ with pairs of vertical dimers. Then we define*

$$w_a(\tilde{\eta}) = w_a(\pi).$$

If there are m odd blocks in $\tilde{\eta}$, then

$$\sum_{\pi \text{ fills in } \tilde{\eta}} w_a(\pi) = (1 + q_0^{a+1} q_1^a)^m w_a(\tilde{\eta}) \quad (2.5)$$

because each odd block of $\tilde{\eta}$ may be filled in two ways: we can use two vertical dimers (which each have weight 1) or we can use two horizontal dimers (which have a combined weight of $q_0^{a+1} q_1^a$ by Lemma 2.4.2). Similarly, if there are m' odd blocks in $S(\tilde{\eta})$, we have

$$\sum_{\pi' \text{ fills in } S(\tilde{\eta})} w_{a+1}(\pi') = (1 + q_0^{a+1} q_1^a)^{m'} w_{a+1}(S(\tilde{\eta})) \quad (2.6)$$

As $\tilde{\eta}$ runs over $\tilde{\mathcal{P}}_n$, $S(\tilde{\eta})$ runs over $\widehat{\mathcal{P}}_{n+1}$. Also, Lemma 2.2.6 implies that $m - m' = n$, so combining Equations (2.5) and (2.6), we get

$$\sum_{\pi \in \mathcal{P}_n} w_a(\pi) = (1 + q_0^{a+1} q_1^a)^n \sum_{\pi \in \mathcal{P}_{n+1}} w_{a+1}(\pi) \quad (2.7)$$

Using Equation (2.7) k times, starting with $n = 1$ and $a = 0$, yields

$$Z(1; q_0, q_1) = \left(\prod_{i=1}^k (1 + q_0^i q_1^{i-1})^i \right) \sum_{\pi \in \mathcal{P}_{k+1}} w_k(\pi). \quad (2.8)$$

As $k \rightarrow \infty$, the product on the right-hand side becomes $M(-q_1^{-1}, q_0 q_1)^{-1}$, which is certainly good news, as this is one of the factors which appears in the statement of Theorem 2.1.5. Next we need to try to understand the sum

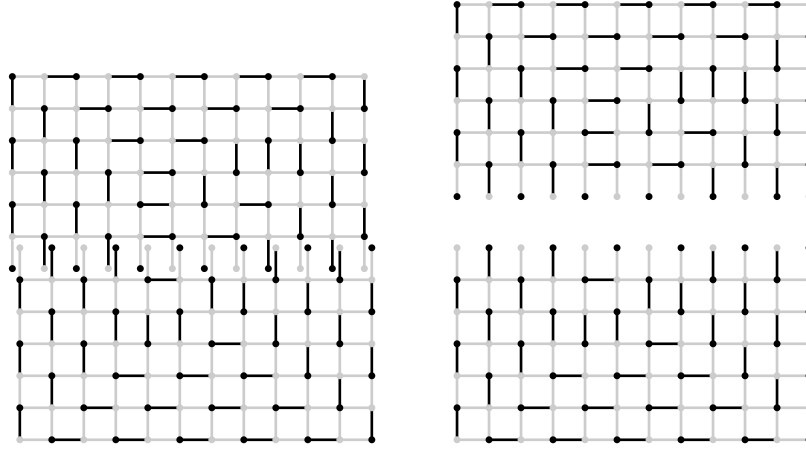
$$\sum_{\pi \in \mathcal{P}_{k+1}} w_k(\pi)$$

in the limit $k \rightarrow \infty$.

2.5 Length- ∞ pyramid partitions

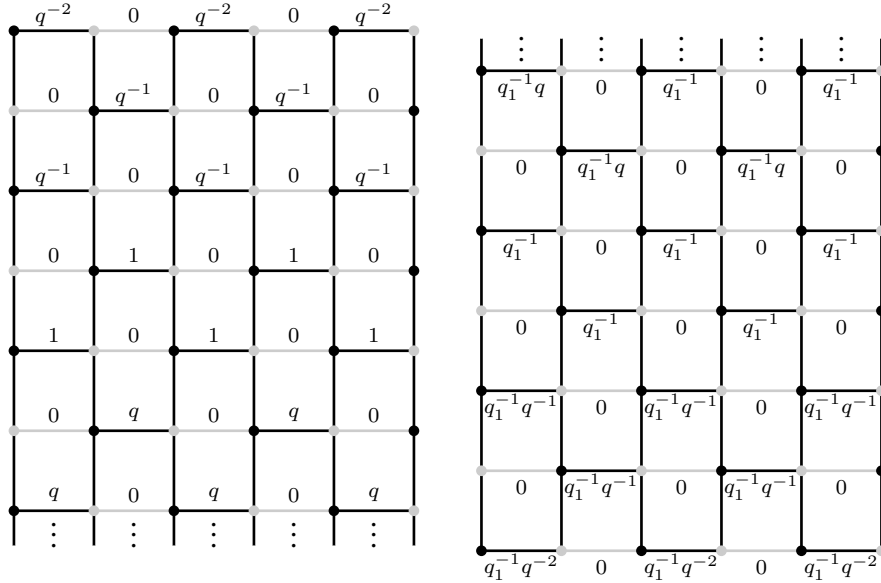
In order to speak sensibly about the limit of the weighting functions w_n as n gets large, we must shift our viewpoint slightly. We shall split the square lattice along the x axis, giving us two half planes. There are infinitely many vertical edges which cross the x axis; we shall include these edges in both half-planes, and identify them. A pyramid partition of length 1 therefore corresponds to two half-pyramid partitions which agree along the “ragged” edges of the two half-planes (see Figure 2.9). Note that we don’t quite have two matchings of the two graphs because the edges which cross the x axis are not necessarily in π .

Figure 2.9: A pyramid partition, being split into two pieces which agree along the seam.



This is a trivial change of viewpoint, but it allows us to shuffle the upper and lower half-planes independently. When we are applying S to the weights in the lower half-plane, let us imagine that we are travelling with the southbound weights. From our new point of view, the northbound weights now move two units north, the “westbound” weights move northwest, and the “eastbound” weights move northeast. Similarly, when we are applying S to the upper half-plane, we are travelling with the northbound weights.

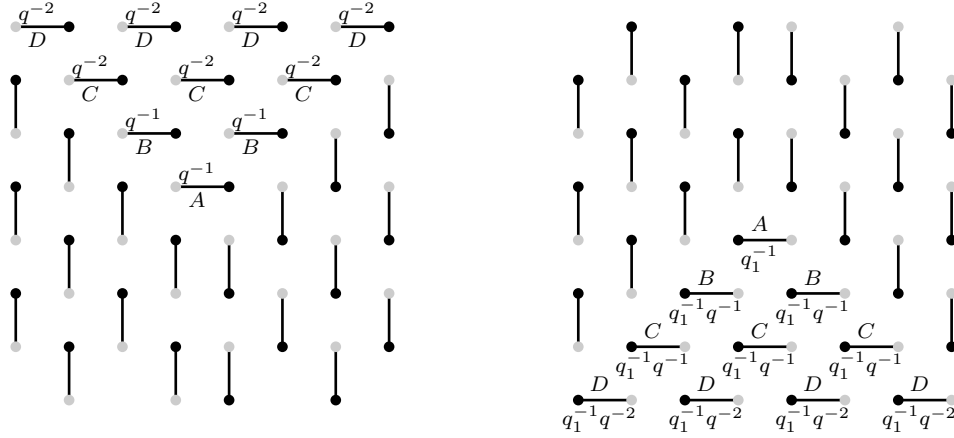
Now it is clear what happens to the weight function w_n as n goes to infinity. In the lower half-plane, nothing happens to the (now stationary) southbound edges at all. However, the weights of the northbound edges get multiplied by q_0q_1 . Let $q = q_0q_1$. If we start with $n = 1$ and shuffle k times, the northbound edges are multiplied by q^n . As $n \rightarrow \infty$, $q^n \rightarrow 0$ in the ring of formal power series, so these

Figure 2.10: The weighting w_∞ , top and bottom pieces.

edges get weight zero. In the same way, the southbound edges in the upper half plane get weight zero. We call this weight function w_∞ ; it is shown in Figure 2.10.

We compute the weights of pyramid partitions in the same way as before: by normalizing by the weight of ε_∞ (see Figure 2.11). When we compute the sum $\sum_\pi w_\infty(\pi)$, we find that pyramid partitions with southbound edges in the upper part, or northbound edges in the lower part, get assigned weight zero. Therefore, the only configurations π that contribute to the sum $\sum w_\infty(\pi)$ are in fact perfect matchings on the heavy edges in Figure 2.10, asymptotically identical to the empty room of length infinity (see Figure 2.11).

Furthermore, if a dimer configuration of this type has horizontal edges arbitrarily far south in its upper half, or arbitrarily far north in its lower half, it also gets weight zero. Thus the only dimer configurations that get nonzero weight un-

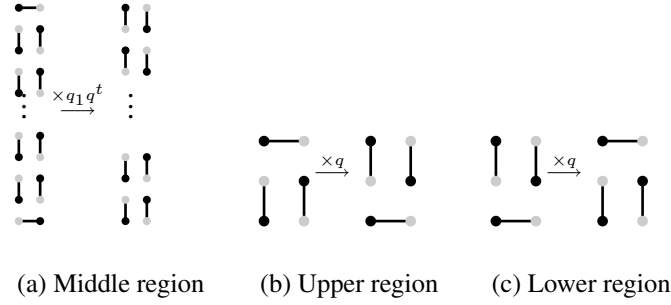
Figure 2.11: The empty room of length ∞ , ε_∞ , top and bottom halves

der w_∞ have a large frozen region of vertical dimers in the northern region of the bottom half, and a corresponding region in the southern region of the top half.

Definition 2.5.1 A pyramid partition of length ∞ is a dimer configuration π with $w_\infty(\pi) > 0$.

In order to determine whether pyramid partitions of length ∞ can be weight-enumerated in any sensible way, we should try to write down a set of elementary moves which can be applied to the empty room, sequentially, and are capable of generating all such π . One such set is depicted in Figure 2.12. Moves of type (b) and (c) may be applied anywhere in the north and south regions of the diagram, respectively; move (a) alters an entire column of vertical dimers which crosses from the top half of the pyramid partition to the bottom half; t indicates how far from the origin the endpoints of the column lie.

One uses these elementary moves as follows. Suppose we wish to construct a partition $\pi \in \mathcal{P}_\infty$. Start with ε_∞ , and apply the “infinite” elementary move (a)

Figure 2.12: Elementary moves for generating elements of \mathcal{P}_∞ from ε_∞ 

until the frozen region in the middle is correct. Then apply move (b) to the upper region and move (c) to the lower region until you have π .

Note that move (a) deletes horizontal dimers from ε_∞ symmetrically in pairs. The first application of the move deletes the two dimers marked A in Figure 2.11; the next deletes two dimers marked B , and so on. Furthermore, the weight change of move (a) depends on where it is applied. If two dimers marked A are deleted, then the weight increases by $q_1 q$; if two dimers marked B are deleted, then the weight increases by $q_1 q^2$, and so on.

2.6 A weight-preserving bijection

We begin by defining super-rigid partitions, which are so named because they are a class of three-dimensional partitions whose generating function is the partition function for the Donaldson-Thomas theory of Calabi-Yau threefolds which come from super-rigid rational curves (see [1]). We recall their definitions and lemma:

Definition 2.6.1 A super-rigid partition is a triple $(\pi_0, \lambda, \pi_\infty)$, where π_0 and π_∞

are three-dimensional partitions sharing a common infinitely long leg of boxes, whose cross-section is a (2-dimensional) Young diagram of shape λ (see Figure 2.13).

Lemma 2.6.2 (Lemma 2.9 of [1]) *Assign to the super-rigid partition $(\pi_0, \lambda, \pi_\infty)$ the weight $z^{|\lambda|} q^{N(\pi_0, \lambda, \pi_\infty)}$, where*

$$N(\pi_0, \lambda, \pi_\infty) = N = |\pi_0| + |\pi_\infty| + \sum_{i,j \in \lambda} (i + j + 1).$$

The generating function for super-rigid partitions under this weighting scheme is

$$Z_X(z, q) = M(1, q)^2 M(-z, q)^{-1};$$

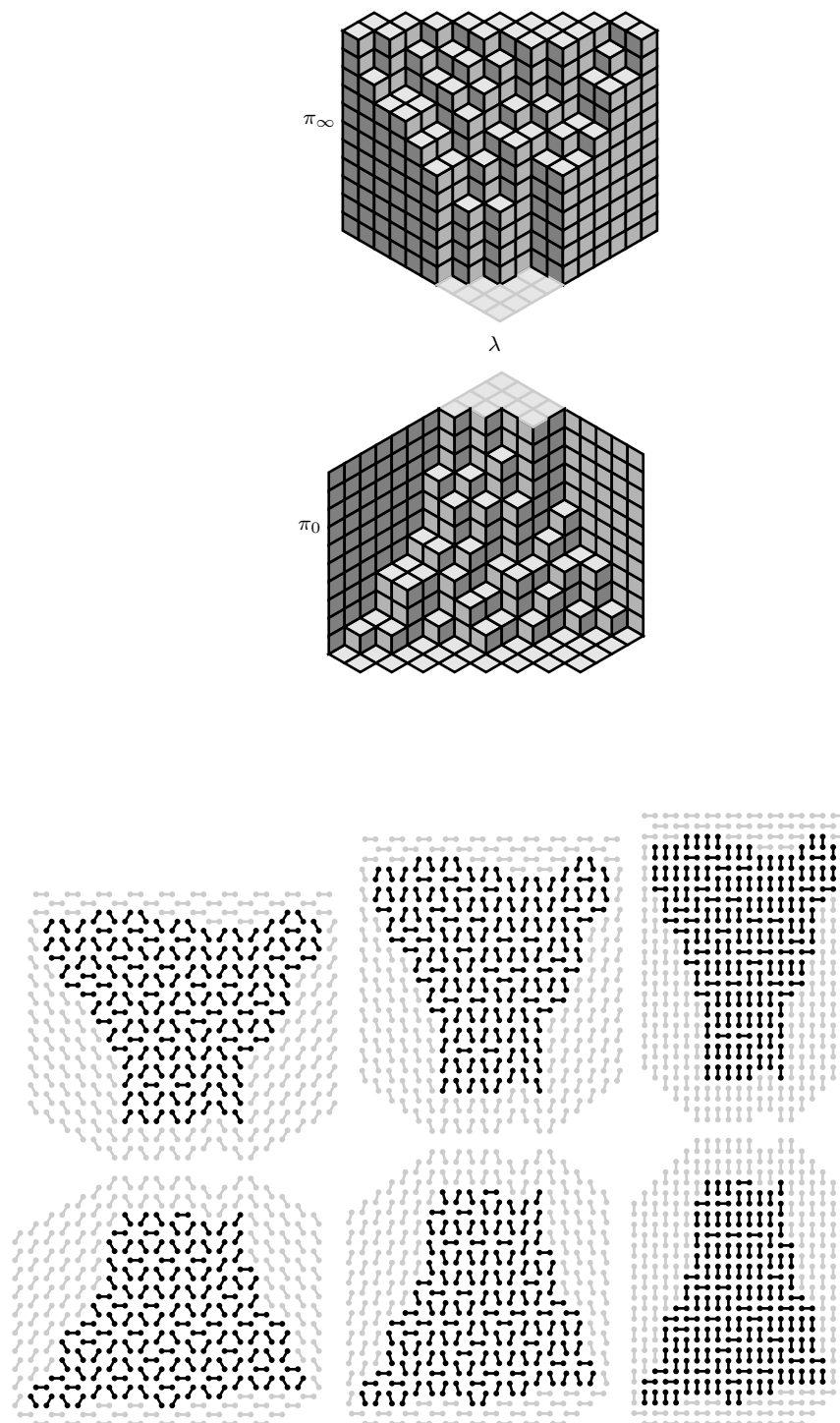
The following is an immediate consequence of Lemma 2.6.2 and of Definition 2.1.4:

Lemma 2.6.3 $Z(\infty; q_0, q_1) = Z_X(q_1, q_0 q_1)$.

There is a “folklore” correspondence between 3D partitions and dimer covers of the hexagon lattice [4]: if we view a 3D partition from far away along the line $x = y = z$, it appears to be a tiling of the plane by lozenges. Replacing each of these lozenges with a dimer, we get a dimer cover of the hexagon lattice. A simple reorientation of the edges of the hexagon lattice shows that it is the same as the “brickwork” lattices defined by the heavy lines of Figure 2.10.

Let us apply this observation to create a correspondence between super-rigid partitions and pyramid partitions of length ∞ . Starting with $(\pi_0, \lambda, \pi_\infty)$, replace both π_0 and π_∞ by their dimer versions, and then reorient all of the edges so that the dimers fit onto the brickwork lattice (see Figure 2.13). The fact that π_0 and π_∞ share a common asymptotic leg λ causes the frozen region of vertical dimers

Figure 2.13: A super-rigid partition $(\pi_0, \lambda, \pi_\infty)$ redrawn as a pyramid partition of length ∞



to appear in the middle of the figure. The correspondence is clearly bijective, and with a little care, we can make this bijection weight-preserving.

Consider any super-rigid partition $(\pi_0, \lambda, \pi_\infty)$. We can construct this partition from the empty super-rigid partition $(\emptyset, \emptyset, \emptyset)$ using the following three elementary moves:

- (a) Add a line of boxes in position (i, j) to the asymptotic leg, with weight $q_1 q^{i+j+1}$. Repeat until we have constructed λ .
- (b) Add a box to the left end of the partition, with weight q . Repeat until we have constructed the super-rigid partition $(\pi_0, \lambda, \emptyset)$.
- (c) Add a box to the right end of the partition, with weight q . Repeat until we have constructed $(\pi_0, \lambda, \pi_\infty)$.

A partition constructed in this manner will be weighted correctly to contribute to $Z(\infty; q_0, q_1)$. Note that we have deliberately chosen these moves to have the same names as those in Figure 2.12. Define a bijection

$$\Phi : \mathcal{P}_\infty \rightarrow \{\text{super-rigid partitions}\}$$

as follows: given $\pi \in \mathcal{P}_\infty$, determine a set of elementary moves to construct π from ε_∞ , and then use the corresponding moves in the same order to create a super-rigid partition. This super-rigid partition is $\Phi(\pi)$.

Since each of these elementary moves affects the weight in the same manner as the corresponding move on pyramid partitions, Φ is weight-preserving. Thus Φ also preserves the generating functions:

$$\sum_{\pi \in \mathcal{P}_\infty} w_\infty(\pi) = Z(\infty; q_0, q_1).$$

In the limit $n \rightarrow \infty$, Equation 2.8 now says

$$Z(1; q_0, q_1) = \left(\prod_{i=1}^{\infty} (1 + q_0^i q_1^{i-1})^i \right) Z(\infty; q_0, q_1)$$

which proves Theorem 2.1.5.

2.7 The generating function for general n

Next, we shall use the same argument to calculate $Z(n; q_0, q_1)$. Applying Equation (2.7) k times, starting at $a = 0$ but leaving n arbitrary, we get

$$Z(n; q_0, q_1) = \left(\prod_{i=1}^k (1 + q_0^i q_1^{i-1})^{i+n-1} \right) \sum_{\pi \in \mathcal{P}_{k+n}} w_k(\pi). \quad (2.9)$$

Taking the limit as k approaches infinity, we again get a sum over pyramid partitions of length ∞ , but with a slightly modified weight function w_∞^n :

$$Z_n(; q_0, q_1) = \left(\prod_{i=1}^{\infty} (1 + q_0^i q_1^{i-1})^{i+n-1} \right) \sum_{\pi \in \mathcal{P}_\infty} w_\infty^n(\pi), \quad (2.10)$$

w_∞^n has the property that the elementary move of type (a) carries the weight $q_1 q^{i+j+n}$. This means that the corresponding super-rigid partition $(\pi_0, \lambda, \pi_\infty)$ has weight $q_1^{|\lambda|} q^{N(n)}$, where

$$N(n) = |\pi_0| + |\pi_\infty| + (n-1)|\lambda| + \sum_{i,j \in \lambda} (i+j+1).$$

We only need a slight modification to the argument of [1] to compute the sum on the right-hand side of Equation 2.10. We begin with the one-leg formula for the topological vertex (see [5]), which states that

$$\sum_{\pi \text{ asymp. to } \lambda} q^{|\pi|} = M(q) q^{\binom{\lambda}{2}} s_{\lambda'}(q), \quad (2.11)$$

where $\binom{\lambda}{2} = \sum_{\lambda_i \in \lambda} \binom{\lambda_i}{2}$, λ' denotes the transpose of λ , and $s_{\lambda'}(q)$ denotes the principal specialization $x_i = q^{i-1}$ of the Schur function $s_{\lambda'}(x_1, x_2, \dots)$. Applying (2.11) twice, we have

$$\begin{aligned}
\sum_{\pi \in \mathcal{P}_\infty} w_\infty^n(\pi) &= \sum_{\lambda} \sum_{\pi_1, \pi_\infty \rightarrow \lambda} q^{N(n)} q_1^{|\lambda|} \\
&= M(1, q)^2 \sum_{\lambda} q_1^{|\lambda|} q^{(n-1)|\lambda| + \binom{\lambda}{2} + \binom{\lambda^t}{2} + \sum_{(i,j) \in \lambda} i+j-1} s_{\lambda^t}(q) s_{\lambda}(q) \\
&= M(1, q)^2 \sum_{\lambda} q_1^{|\lambda|} q^{n|\lambda|} s_{\lambda^t}(q) s_{\lambda}(q) \\
&= M(1, q)^2 \prod_{i,j=1}^{\infty} (1 + q_1 q^{i+j+n-2}) \\
&= M(1, q)^2 \prod_{k=1}^{\infty} (1 + q_0^k q_1^{k+1})^{\max(k-n+1, 0)}.
\end{aligned}$$

This proves Theorem 2.2. □

2.8 Conclusion

There are two obvious applications of the computational techniques of this paper, which we will pursue in future work:

1. The shuffling procedure still works for certain pyramid partitions which are not asymptotic to ε_n . In particular, we can allow pyramid partitions to have up to four asymptotic legs, pointing NW, NE, SW, and SE, whose shapes are given by partitions $\lambda_{NW}, \lambda_{NE}, \lambda_{SW}, \lambda_{SE}$. It seems possible that we could compute the generating function for such configurations using the full topological vertex formula of [5]. Such a result might shed some light on flop transitions in topological string theory.

2. It may be possible to compute a somewhat more refined generating function, using $2n$ variables rather than just two. This would have the effect of introducing diagonal “stripes” on the alternate layers of the pyramid partition. Such a count may be related to the partition functions of orbifold Donaldson-Thomas theory (see Chapter 3).

The geometric value of both of these approaches is unclear at best; let us be conservative and say that they would be good combinatorial exercises. One interesting hint of geometry which has arisen from this paper, however, is the direct link between the Donaldson-Thomas partition function of the conifold, $Z(1, q_0, q_1)$, and the Donaldson-Thomas partition function of the resolution, $Z(\infty, q_0, q_1)$. We have observed a similar coincidence in the DT partition functions of orbifolds and their resolutions (see the Appendix).

Acknowledgements

The author would like to thank Dr. Balázs Szendrői for posing this problem, and Dr. Richard Kenyon for a fruitful conversation which led to its solution.

Bibliography

- [1] Kai Behrend and Jim Bryan. Super-rigid Donaldson-Thomas invariants, 2006.
- [2] Noam Elkies, Greg Kuperberg, Michael Larsen, and James Propp. Alternating sign matrices and domino tilings ii. *Journal of Algebraic Combinatorics*, 1(3):219–234, November 1992.
- [3] Richard Kenyon. Talk at the workshop on random partitions and Calabi-Yau crystals, Amsterdam, 2005. Available at <http://www.math.brown.edu/~rkenyon/talks/pyramids.pdf>.
- [4] Richard Kenyon. Height fluctuations in the honeycomb dimer model. Preprint: arXiv:math-ph/0405052v2, May 2007.
- [5] Andrei Okounkov, Nikolai Reshetikhin, and Cumrun Vafa. Quantum Calabi-Yau and classical crystals. *Progress in Mathematics*, 244:597–618, November 2006.
- [6] Balázs Szendrői. Non-commutative Donaldson-Thomas theory and the conifold. To appear in *Geometry and Topology*. arXiv:0705.3419v1 [math.AG].

Chapter 3

Counting 3D Young diagrams with vertex operators

3.1 Introduction

A *3D Young diagram*, or *3D diagram* for short, is a stable pile of cubical boxes which sit in the corner of a large cubical room. More formally, a 3D Young diagram is a finite subset π of $(\mathbb{Z}_{\geq 0})^3$ such that if any of

$$(i+1, j, k), (i, j+1, k), (i, j, k+1)$$

are in π , then $(i, j, k) \in \pi$. The ordered triples are the “boxes”; the closure condition means that the boxes of a 3D partition are stacked stably in the positive octant, with gravity pulling them in the direction $(-1, -1, -1)$.

3D Young diagrams are well-studied; they are also called *plane partitions* or *3D partitions* elsewhere in the literature. The first result on 3D Young diagrams is due to Dr. Percy MacMahon [6]. MacMahon was the first to “ q -count” (i.e. to give a generating function for) 3D Young diagrams by volume:

$$\sum_{\pi \text{ 3D diagram}} q^{|\pi|} = \prod_n \left(\frac{1}{1 - q^n} \right)^n, \quad (3.1)$$

where $|\pi|$ denotes the number of boxes in π . Generating functions of this form will appear frequently, so we adopt the following notation:

Definition 3.1.1 *Let*

$$M(x, q) = \prod_{i=1}^n \left(\frac{1}{1 - xq^n} \right)^n$$

$$\widetilde{M}(x, q) = M(x, q)M(x^{-1}, q)$$

⁰A version of this chapter has been submitted for publication. Young, B., with an appendix by Bryan, J. Generating functions for colored 3D Young diagrams and the Donaldson-Thomas invariants of orbifolds.

We call $M(x, q)$ and $\widetilde{M}(x, q)$ the *MacMahon* and *MacMahon tilde* functions, respectively. Strictly speaking, $\widetilde{M}(x, q)$ lies in the ring of formal power series $\mathbb{Z}[[x, x^{-1}, q]]$. However, in all of our applications, we will specialize x and q in such a way that no negative powers of any variables appear in the formulae (see Theorems 3.1.4 and 3.1.5).

Since MacMahon, there have been many proofs of (3.1), spanning many fields: combinatorics, statistical mechanics, representation theory, and others. Recently, there has been a thorough study of the various symmetry classes of 3D Young diagrams [2], and of many macroscopic properties of large random 3D Young diagrams [9]. There is also active research in algebraic geometry which relies upon enumerations of various types of 3D partitions [7].

We will derive two refinements of MacMahon’s generating function. Fix a set of colours \mathcal{C} , and replace the variable q with a set of variables,

$$\mathcal{Q} = \{q_g \mid g \in \mathcal{C}\}.$$

We call \mathcal{C} the set of “colours”. We will need to assign a colour to each point of the first orthant. In particular, we will usually have $\mathcal{C} = G$, a finite Abelian group. In this case, addition in $\mathbb{Z}_{\geq 0}^3$ must respect the group law of G .

Definition 3.1.2 *A colouring is a map*

$$K : (\mathbb{Z}_{\geq 0})^3 \rightarrow \mathcal{C}.$$

If $\mathcal{C} = G$ is a finite Abelian group, then a G -colouring is a colouring which is also a homomorphism of additive monoids.

Note that a G -colouring is uniquely determined by $K(1, 0, 0)$, $K(0, 1, 0)$ and $K(0, 0, 1)$, and that $K(0, 0, 0)$ is the identity element of G .

There is a simple way of defining a G -colouring K_G when G is a three-dimensional matrix group. Decompose G as a direct sum of one-dimensional representations R_x, R_y, R_z . The set of irreducible representations of any Abelian G forms a group $\widehat{G} \simeq G$ under tensor product, so let ψ be an isomorphism $\psi : \widehat{G} \longrightarrow G$ and define

$$K_G(i, j, k) = \psi(R_x^{\otimes i} \otimes R_y^{\otimes j} \otimes R_z^{\otimes k}).$$

Both of the colourings used in this paper are of this form.

We next define the multivariate generating function $Z_G = Z_G(\mathcal{Q})$ which “ \mathcal{Q} -counts” diagrams (that is, Z_G counts each diagram with the \mathcal{Q} -weight of its boxes):

Definition 3.1.3 For $g \in G$, let $|\pi|_g$ be the number of g -coloured boxes in π ,

$$|\pi|_g = |K_G^{-1}(g) \cap \pi|.$$

Define the G -coloured partition function

$$Z_G = \sum_{\pi \text{ 3D partition}} \prod_{g \in G} q_g^{|\pi|_g}.$$

The question of determining Z_G , though completely combinatorial, has its genesis in a field of enumerative algebraic geometry called *Donaldson-Thomas theory*. When G is a finite Abelian subgroup of $SO(3)$ (which forces $G = \mathbb{Z}_n$ or $\mathbb{Z}_2 \times \mathbb{Z}_2$), there is a colouring induced by the natural three dimensional representation for which the generating function Z_G is, up to signs of the variables, the orbifold Donaldson–Thomas partition function for the quotient stack $[\mathbb{C}^3/G]$ (see Appendix A). Although it is not yet clear why, these seem to be precisely the groups G for which Z_G has a product formula.

Theorem 3.1.4 *Let $G = \mathbb{Z}_n$ and let the colouring $K_{\mathbb{Z}_n}$ be given by*

$$K_{\mathbb{Z}_n}(1, 0, 0) = 1$$

$$K_{\mathbb{Z}_n}(0, 1, 0) = -1$$

$$K_{\mathbb{Z}_n}(0, 0, 1) = 0.$$

Let $q = q_0 \cdots q_{n-1}$ and for $a, b \in [1, n-1]$, let $q_{[a,b]} = q_a q_{a+1} \cdots q_b$. Then

$$Z_{\mathbb{Z}_n} = M(1, q)^n \prod_{0 < a \leq b < n} \widetilde{M}(q_{[a,b]}, q).$$

The proof of Theorem 3.1.4 is straightforward; it is essentially a simple modification of the methods used in [11]. We include it for completeness and as an introduction to the vertex operator calculus used to prove Theorem 3.1.5. There are several other ways to prove Theorem 3.1.4, some of which have (at least implicitly) appeared in the literature. For example, [1, 4] both compute a generating function with variables $x_k (k \in \mathbb{Z})$ which can be easily specialized to $Z_{\mathbb{Z}_n}$. The result [1] is particularly notable, as it is a direct computer algebra implementation of MacMahon's techniques of combinatorial analysis. The following theorem, however, is new:

Theorem 3.1.5 *Let $G = \mathbb{Z}_2 \times \mathbb{Z}_2 = \{0, a, b, c\}$ and let the colouring $K_{\mathbb{Z}_2 \times \mathbb{Z}_2}$ be given by*

$$K_{\mathbb{Z}_2 \times \mathbb{Z}_2}(1, 0, 0) = a$$

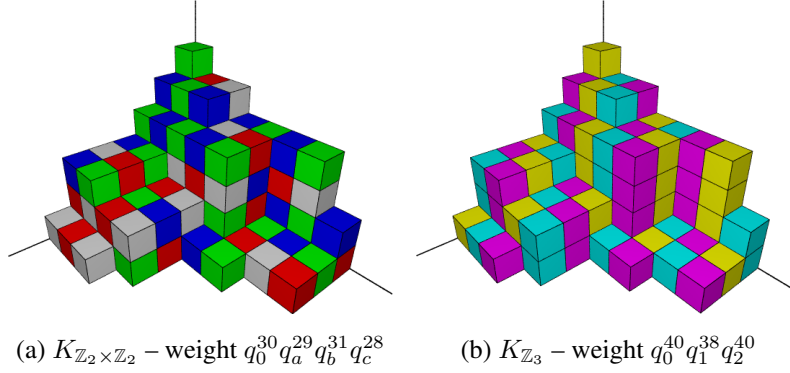
$$K_{\mathbb{Z}_2 \times \mathbb{Z}_2}(0, 1, 0) = b$$

$$K_{\mathbb{Z}_2 \times \mathbb{Z}_2}(0, 0, 1) = c.$$

Let $q = q_0 q_a q_b q_c$. Then

$$Z_{\mathbb{Z}_2 \times \mathbb{Z}_2} = M(1, q)^4 \cdot \frac{\widetilde{M}(q_a q_b, q) \widetilde{M}(q_a q_c, q) \widetilde{M}(q_b q_c, q)}{\widetilde{M}(-q_a, q) \widetilde{M}(-q_b, q) \widetilde{M}(-q_c, q) \widetilde{M}(-q_a q_b q_c, q)}.$$

Figure 3.1: A partition coloured according to $K_{\mathbb{Z}_2 \times \mathbb{Z}_2}$ and to $K_{\mathbb{Z}_3}$



See Figure 3.1 for pictures of a partition coloured in the manner described by these theorems.

As an application of these theorems, we will compute the Donaldson-Thomas invariants of the orbifolds $[\mathbb{C}^3/\mathbb{Z}_n]$ and $[\mathbb{C}^3/\mathbb{Z}_2 \times \mathbb{Z}_2]$. The orbifold Donaldson-Thomas partition function of $[\mathbb{C}^3/G]$ has variables labeled by representations of G (see Appendix) and hence has the same variables as the G -coloured diagram partition function. In the Appendix, we prove that the diagram partition function and the Donaldson-Thomas partition function are related by simple sign changes on the variables:

Theorem 3.1.6 *The orbifold Donaldson-Thomas partition functions of the orbifolds $[\mathbb{C}^3/\mathbb{Z}_2 \times \mathbb{Z}_2]$ and $[\mathbb{C}^3/\mathbb{Z}_n]$ are given by*

$$Z_{\mathbb{C}^3/\mathbb{Z}_n}^{DT}(q_0, q_1, \dots, q_{n-1}) = Z_{\mathbb{Z}_n}(-q_0, q_1, \dots, q_{n-1})$$

$$Z_{\mathbb{C}^3/\mathbb{Z}_2 \times \mathbb{Z}_2}^{DT}(q_0, q_a, q_b, q_c) = Z_{\mathbb{Z}_2 \times \mathbb{Z}_2}(q_0, -q_a, -q_b, -q_c)$$

where q and $q_{[a,b]}$ are defined as in Theorems 3.1.4 and 3.1.5.

There is a striking similarity between the Donaldson-Thomas partition functions of the orbifold $[\mathbb{C}^3/G]$ and the crepant resolution given by the G -Hilbert scheme. The following is proved in the Appendix:

Theorem 3.1.7 *Let $Y_G \longrightarrow \mathbb{C}^3/G$ be the crepant resolution of \mathbb{C}^3/G given by the G -Hilbert scheme. Y_G has a natural basis of curve classes indexed by non-trivial elements of G . The Donaldson-Thomas partition functions of $Y_{\mathbb{Z}_n}$ and $Y_{\mathbb{Z}_2 \times \mathbb{Z}_2}$ are given by*

$$Z_{Y_{\mathbb{Z}_n}}^{DT} = M(1, -q)^n \prod_{0 < a \leq b < n} M(q_{[a,b]}, -q),$$

$$Z_{Y_{\mathbb{Z}_2 \times \mathbb{Z}_2}}^{DT} = M(1, -q)^4 \frac{M(q_a q_b, -q) M(q_b q_c, -q) M(q_a q_c, -q)}{M(q_a, -q) M(q_b, -q) M(q_c, -q) M(q_a q_b q_c, -q)},$$

where $\{q_1, \dots, q_{n-1}\}$ and $\{q_a, q_b, q_c\}$ are the variables corresponding to curve classes and q is the variable corresponding to Euler number.

We see from these theorems that the reduced partition function of the orbifold $[\mathbb{C}^3/G]$ is obtained from the reduced partition function of the resolution by identifying the variables appropriately and then simply writing a tilde over every factor of M in the formula! A similar phenomenon was observed by Szendrői for the partition function of the (non-commutative) conifold singularity and its crepant resolution [13].

It would be very desirable to have even a conjectural understanding of the relationship between the Donaldson-Thomas theory of an arbitrary Calabi-Yau orbifold and its crepant resolution(s). We formulate a conjecture for the case of a local orbifold satisfying the hard Lefschetz condition (see Conjecture A.3.1.

Theorem 3.1.5 is not straightforward to prove. Essentially none of the standard proofs of MacMahon’s colourless result can be modified to work in this situation. The generating function was first conjectured by Jim Bryan based on some related phenomena from Donaldson–Thomas theory; concurrently, Kenyon made an (unpublished) equivalent conjecture for $\mathbb{Z}_2 \times \mathbb{Z}_2$ -weighted dimer models on the hexagon lattice, based on computational evidence.

Having this conjectured formula was crucial for finding the proof of Theorem 3.1.5, which involves a somewhat bizarre detour: one must first \mathcal{Q} -count *pyramid partitions* (see Figure 3.4). One then performs a computation with vertex operators to make $\mathbb{Z}_{\mathbb{Z}_2 \times \mathbb{Z}_2}$ emerge. We discovered this idea serendipitously while trying to generalize our earlier work on pyramid partitions [14].

3.2 Review: the infinite wedge space

Our general strategy will be to think of a 3D diagram π as a set of diagonal slices, $\{\pi_k \mid k \in \mathbb{Z}\}$, where π_k is the set of all bricks which lie in the plane $x - y = k$. We will then analyze how one passes from one slice to the next. Since we will be summing over all 3D Young diagrams, it is very helpful to consider (possibly infinite) formal sums of the form

$$\sum_{\lambda \in \text{some set of partitions}} f_\lambda(\mathcal{Q}) \cdot \lambda,$$

where $f_\lambda(\mathcal{Q})$ is a power series in the elements of \mathcal{Q} . A nice way of describing the set of all such sums is the *charge-zero subspace of the infinite wedge space*,

$$(\Lambda^{\infty/2})_0 V$$

where V is a vector space with a basis labeled by the elements of $\mathbb{Z} + \frac{1}{2}$. This setting allows one to define, quite naturally, several useful operators on partitions.

The use of $(\Lambda^{\infty/2})_0 V$, and its associated operators, was in part popularized by [8, Appendix A], and we shall adhere to the notation established there. In this section, we have collected the minimum number of formulae necessary for our purposes. We will use Dirac's "bra-ket" notation

$$\langle \lambda | \mu \rangle$$

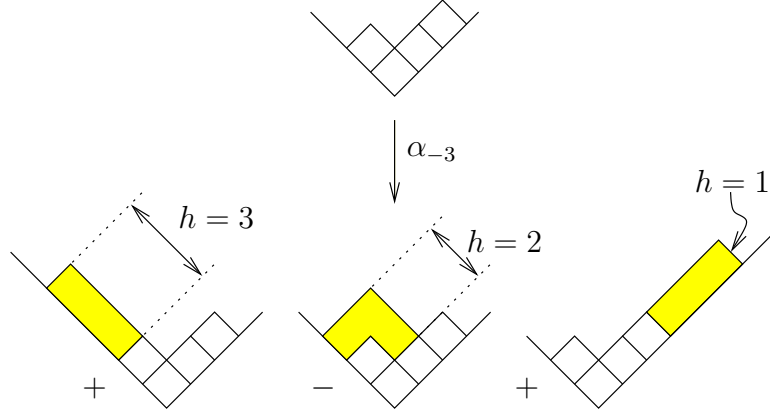
to denote the inner product under which the partitions are orthonormal. We will need the bosonic creation and annihilation operators α_n , defined in [8, Appendix A] in the section on Bosons and Vertex Operators. The operators α_n satisfy the Heisenberg commutation relations,

$$[\alpha_n, \alpha_{-m}] = n\delta_{m,n}. \quad (3.2)$$

Concretely, α_{-n} acts on a 2D Young diagram λ by adding a single border strip of length n onto λ in all possible ways, with sign $(-1)^{h+1}$, where h is the height of the border strip (see Figure 3.2). The operator α_n is adjoint to α_{-n} , and acts by deleting border strips.

Let $x_j (j \geq 1)$ be indeterminates; and define the homogeneous, elementary, and power sum symmetric functions as usual:

$$\begin{aligned} \sum_i h_i(x_1, x_2, \dots) t^i &= \prod_i \frac{1}{1 - x_i t} \\ \sum_i e_i(x_1, x_2, \dots) t^i &= \prod_i (1 + x_i t) \\ p_i(x_1, x_2, \dots) &= \sum_{j \geq 1} x_j^i \end{aligned}$$

Figure 3.2: Applying α_{-3} to a partition

For a comprehensive reference on symmetric functions, see [12]. We next define the vertex operators Γ_{\pm} :

Definition 3.2.1

$$\Gamma_{\pm}(x_1, x_2, \dots) = \exp \sum_k \frac{p_k}{k} \alpha_{\pm k}$$

The matrix coefficients (with respect to the orthonormal basis formed by the 2D Young diagrams) of the Γ_{\pm} operators turn out [8, A.15] to be the skew Schur functions,

$$\langle \lambda | \Gamma_{-}(x_1, x_2, \dots) | \mu \rangle = \langle \mu | \Gamma_{+}(x_1, x_2, \dots) | \lambda \rangle = s_{\lambda/\mu}(x_i).$$

We will need the following well-known theorem from representation theory (see, for example, [3, Chapter 8]) to work with Γ_{\pm} and other exponentiated operators.

Theorem 3.2.2 (*Campbell-Baker-Hausdorff*) *If A and B are operators, then*

$$\log(\exp(A) \exp(B)) = A + B + \frac{1}{2}[A, B] + \dots,$$

where the higher-order terms are multiples of nested commutators of A and B .

It is certainly possible to give more terms in the expansion, but we shall only need the following two corollaries.

Corollary 3.2.3 *If A and B are commuting operators, then*

$$\exp(A) \exp(B) = \exp(A + B).$$

Corollary 3.2.4 *If A and B are operators such that $[A, B]$ is a central element, then we have*

$$\exp(A) \exp(B) = \exp([A, B]) \exp(B) \exp(A).$$

3.3 The operators $\Gamma(x)$, $\Gamma'(x)$, and Q_g

Our next goal is to define precisely what it means for two diagonal slices λ, μ to sit next to one another in a 3D Young diagram, and to define operators for working with such slices.

Definition 3.3.1 *Let λ, μ be two 2D Young diagrams. We say that λ interlaces with μ , and write $\lambda \succ \mu$, if $\mu \subseteq \lambda$ and the skew diagram λ/μ contains no vertical domino.*

For example, $(6, 3, 2) \succ (4, 2)$, because the skew diagram $(6, 3, 2)/(4, 2)$ has no two boxes in the same column. The following lemma is easy to check:

Lemma 3.3.2 *The following are equivalent:*

- I. $\lambda \succ \mu$.

2. The row lengths λ_i, μ_i satisfy $\lambda_1 \geq \mu_1 \geq \lambda_2 \geq \mu_2 \geq \dots$.
3. $\lambda^i - \mu^i = 0$ or 1, for each pair of columns λ^i, μ^i .
4. λ and μ are two adjacent diagonal slices of some 3D Young diagram.

Note that we have used the convenient, but slightly nonstandard, notation λ^i to denote the *columns* of λ .

Part (3) will become relevant in Section 3.5, when we will see that adjacent diagonal slices of a pyramid partition also interlace.

We are mainly interested in two specializations of $\Gamma_{\pm}(x_1, x_2, \dots)$ which create interlacing partitions, and which depend only upon a single indeterminate q . The first will be denoted $\Gamma_{\pm}(q)$, and is obtained by performing the specialization $x_1 \mapsto q, x_i \mapsto 0$ for $i > 1$. Its formula is

$$\Gamma_{\pm}(q) = \exp \sum_k \frac{q^k}{k} \alpha_{\pm k}. \quad (3.3)$$

Recall [12, Chapter 7] that if λ, μ are partitions, then we may define the *skew Schur function* $s_{\lambda/\mu}(x_1, x_2, \dots)$ by $\sum_T x^T$, where T runs over the set of semi-standard tableaux of shape λ/μ . Following [11], we see that

$$s_{\lambda/\mu}(q, 0, 0, \dots) = \begin{cases} q^{|\lambda| - |\mu|} & \text{if } \lambda \succ \mu \\ 0 & \text{if } \lambda \not\succ \mu. \end{cases}$$

One can then show [10] that

$$\Gamma_{-}(q)\mu = \sum_{\lambda \succ \mu} q^{|\lambda| - |\mu|} \lambda \quad \Gamma_{+}(q)\lambda = \sum_{\mu \prec \lambda} q^{|\lambda| - |\mu|} \mu. \quad (3.4)$$

For the second specialization, recall that there is an involution ω on the algebra of symmetric functions [12, Chapter 7.6], given by any one of the following

equivalent definitions:

$$\begin{aligned} e_k(x_i) &\longleftrightarrow h_k(x_i) \\ p_k(x_i) &\longleftrightarrow (-1)^{k-1} p_k(x_i) \\ s_{\lambda/\mu}(x_i) &\longleftrightarrow s_{\lambda'/\mu'}(x_i) \end{aligned}$$

Here, λ' is the transpose partition of λ . To obtain the second specialization, called $\Gamma'_\pm(q)$, we first perform the involution $p_k \mapsto \omega p_k$ and then specialize $x_1 \mapsto q, x_i \mapsto 0$ ($i > 1$) as before. We obtain the formula

$$\Gamma'_\pm(q) = \exp \sum_k \frac{(-1)^{k-1} q^k}{k} \alpha_{\pm k} \quad (3.5)$$

with the property that

$$\Gamma'_-(q)\mu = \sum_{\lambda' \succ \mu'} q^{|\lambda|-|\mu|} \lambda \quad \Gamma'_+(q)\lambda = \sum_{\mu' \prec \lambda'} q^{|\lambda|-|\mu|} \mu.$$

Lemma 3.3.3 *If a and b are commuting variables, then we have the following multiplicative commutators in $\mathbb{C}[[a, b]]$:*

$$\begin{aligned} [\Gamma_+(a), \Gamma'_-(b)] &= 1 + ab & [\Gamma'_+(a), \Gamma_-(b)] &= 1 + ab \\ [\Gamma_+(a), \Gamma_-(b)] &= \frac{1}{1 - ab} & [\Gamma'_+(a), \Gamma'_-(b)] &= \frac{1}{1 - ab} \end{aligned}$$

Proof. Let us compute the first of these commutators; the others are similar. Let us apply (3.2), and then use Corollary 3.2.4 to rephrase the answer as the

exponential of a commutator. We have

$$\begin{aligned}
 [\Gamma'_+(a), \Gamma_-(b)] &= \exp \sum_{j,k} \frac{(-1)^{j-1} a^j b^k}{jk} [\alpha_j, \alpha_{-k}] \\
 &= \exp \left(- \sum_j \frac{(-ab)^j}{j} \right) \\
 &= \exp(\log(1 - (-ab))).
 \end{aligned}$$

□

We next define diagonal operators Q_g for assigning weights to 2D partitions.

Definition 3.3.4 For $g \in G$, define the weight operator Q_g by

$$Q_g |\lambda\rangle = q_g^{|\lambda|} |\lambda\rangle.$$

The operator Q_g can be commuted past any of the Γ_\pm operators, at the expense of changing the argument of Γ_\pm :

$$\begin{aligned}
 \Gamma_+(x)Q_g &= Q_g\Gamma_+(xq_g) & Q_g\Gamma_-(x) &= \Gamma_-(xq_g)Q_g \\
 \Gamma'_+(x)Q_g &= Q_g\Gamma'_+(xq_g) & Q_g\Gamma'_-(x) &= \Gamma'_-(xq_g)Q_g.
 \end{aligned}$$

3.4 Counting with Z_n colouring

As a motivating example, let us use (3.4) to write down a vertex operator expression which computes MacMahon's generating function (3.1), using the variable $q = q_0$. This formula appears in [11] with marginally different notation.

Consider a 3D Young diagram π and its diagonal slices:

$$\phi \prec \cdots \prec \pi_{-2} \prec \pi_{-1} \prec \pi_0 \succ \pi_1 \succ \pi_2 \succ \cdots \succ \phi,$$

where ϕ denotes the empty partition. Each such π contributes

$$q_0^{|\pi|} = q_0^{\sum |\pi_n|}$$

to the generating function, so we have

$$\sum_{\pi \text{ 3D diagram}} q^{|\pi|} = \left\langle \phi \left| \prod_{i=1}^{\infty} (\Gamma_+(1)Q_0) \prod_{i=1}^{\infty} (\Gamma_-(1)Q_0) \right| \phi \right\rangle.$$

This works because the operators Γ_- and Γ_+ pass from one slice to the next larger (respectively smaller) slice in all possible ways, and the Q_0 operators assign the proper weight to each slice. One then commutes all the Γ_- operators to the left and all the Γ_+ operators to the right (following the method outlined in [11]) to compute the generating function.

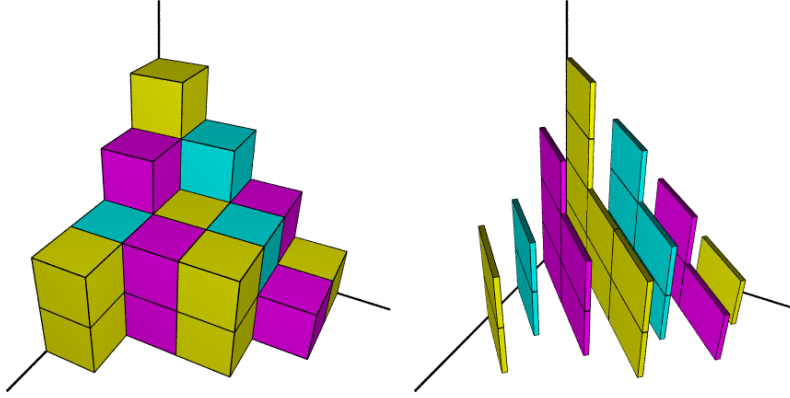
Let us now write down a vertex operator expression which computes $Z_{\mathbb{Z}_n}$. Here, $\mathcal{Q} = \{q_0, \dots, q_{n-1}\}$, $q = q_0 q_1 \cdots q_{n-1}$, and $K = K_{\mathbb{Z}_n}$. The computation is straightforward (following precisely the method of [11]) but awkward, so it is helpful to organize the work by collecting together n vertex operators at a time. Note that the diagonal slices of π are all monochrome (see Figure 3.3), so we define

$$\overline{A}_{\pm}(x) = \Gamma_{\pm}(x)Q_1\Gamma_{\pm}(x)Q_2 \cdots Q_{n-1}\Gamma_{\pm}(x)Q_0$$

Then, the following vertex operator product counts \mathbb{Z}_n -coloured 3D diagrams:

$$Z_{\mathbb{Z}_n} = \langle \phi | \cdots \overline{A}_+(1)\overline{A}_+(1)\overline{A}_+(1)\overline{A}_-(1)\overline{A}_-(1)\overline{A}_-(1) \cdots | \phi \rangle \quad (3.6)$$

Let $q = q_0 q_1 \cdots q_{n-1}$, and let $Q = Q_0 Q_1 \cdots Q_{n-1}$. We use the commutation

Figure 3.3: Slicing a \mathbb{Z}_3 -coloured 3D diagram

relations of the previous section to compute

$$\begin{aligned}
 \overline{A}_+(x) &= Q \cdot \Gamma_+(xq_1q_2q_3 \cdots q_{n-1}q_0) \Gamma_+(xq_2q_3 \cdots q_{n-1}q_0) \cdots \Gamma_+(xq_0) \\
 \overline{A}_-(x) &= \Gamma_+(x)\Gamma_+(xq_1) \cdots \Gamma_+(xq_1q_2 \cdots q_{n-1}) \cdot Q \\
 &= \Gamma_+(xqq_1^{-1}q_2^{-1} \cdots q_{n-1}^{-1}q_0^{-1}) \Gamma_+(xqq_2^{-1}q_3^{-1} \cdots q_{n-1}^{-1}q_0^{-1}) \cdots \\
 &\quad \cdots \Gamma_+(xqq_0^{-1}) \cdot Q
 \end{aligned}$$

Next, set

$$A_+(x) = Q^{-1}\overline{A}_+(x); \quad A_-(x) = \overline{A}_-(x)Q^{-1}.$$

From this expression, it is clear that

$$A_+(x)A_-(y) = C(x, y) \cdot A_-(y)A_+(x)$$

where $C(x, y)$ is the following product of the n^2 commutators obtained by moving

a Γ_+ past a Γ_- :

$$C(x, y) = \left(\frac{1}{1 - qxy} \right)^n \prod_{0 \leq a \leq b < n} \left(\frac{1}{1 - (q_a q_{a+1} \cdots q_b) qxy} \right) \\ \cdot \prod_{0 \leq a \leq b < n} \left(\frac{1}{1 - (q_a q_{a+1} \cdots q_b)^{-1} qxy} \right)$$

We now follow the derivation of MacMahon's formula in [11]. Starting with (3.6), we convert all of the \bar{A}_\pm into A_\pm and move the resulting weight functions to the outside of the product (where they act trivially). This gives

$$Z_{\mathbb{Z}_n} = \langle \phi | \cdots A_+(q^2) A_+(q) A_+(1) A_-(1) A_-(q) A_-(q^2) \cdots | \phi \rangle.$$

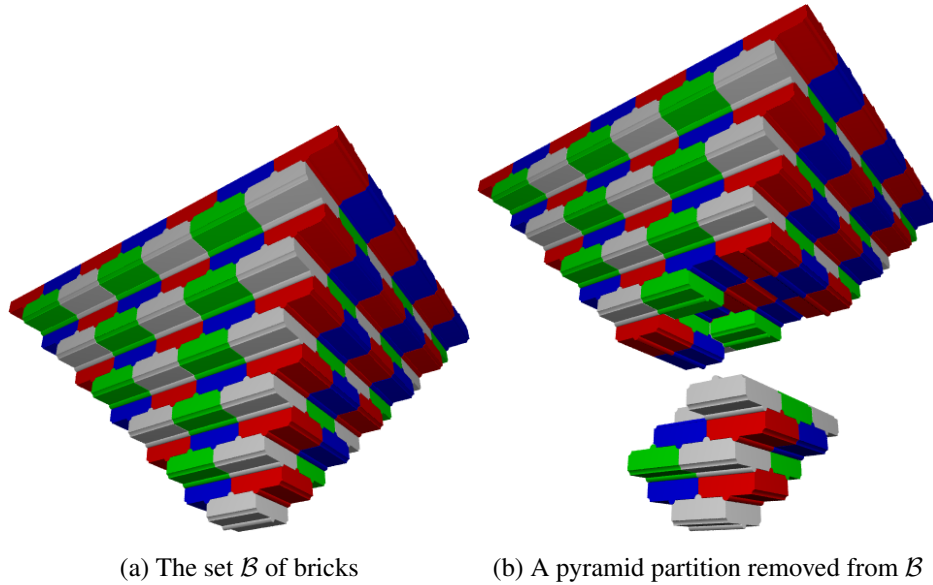
We then commute all A_+ operators to the right and all A_- to the left:

$$\begin{aligned} Z_{\mathbb{Z}_n} &= \langle \phi | \cdots A_+(q^2) A_+(q) \underbrace{A_+(1) A_-(1)} \underbrace{A_-(q) A_-(q^2)} \cdots | \phi \rangle \\ &= C(1, 1) \left\langle \phi \left| \cdots A_+(q^2) \underbrace{A_+(q) A_-(1) A_+(1) A_-(q)} A_-(q^2) \cdots \right| \phi \right\rangle \\ &= \cdots \\ &= \prod_{i,j=0}^{\infty} C(q^i, q^j) \cdot \langle \phi | A_-(1) A_-(q) A_-(q^2) \cdots A_+(q^2) A_+(q) A_+(1) | \phi \rangle. \end{aligned}$$

The vertex operator product in the final line is now equal to 1, because $\langle \phi | A_-(x) = \langle \phi |$ and $A_+(x) | \phi \rangle = | \phi \rangle$. Finally, we rewrite the remaining product with MacMahon functions:

$$\begin{aligned} Z_{\mathbb{Z}_n} &= \prod_{i,j=0}^{\infty} C(q^i, q^j) \\ &= M(1, q)^n \prod_{0 \leq a \leq b < n} M(q_a \cdots q_b, q) M(q_a^{-1} \cdots q_b^{-1}, q) \\ &= M(1, q)^n \prod_{0 \leq a \leq b < n} \widetilde{M}(q_a \cdots q_b, q), \end{aligned}$$

Figure 3.4

(a) The set \mathcal{B} of bricks(b) A pyramid partition removed from \mathcal{B}

and Theorem 3.1.4 is proven. \square

3.5 Pyramid partitions

The methods of the Section 3.4 may also be used to \mathcal{Q} -count a similar type of three-dimensional combinatorial object, called *pyramid partitions*. Essentially, we want to replace $\mathbb{Z}_{\geq 0}^3$ with the upside-down pyramid shaped stack of bricks shown in Figure 3.4. Note that the bricks have ridges and grooves set into them; this helps to remind us how the bricks are meant to stack.

Szendrői [13] introduced us to the ideas in this section, albeit in a different context. He proves that counting pyramid partitions with a slightly simpler colour

scheme (namely specializing $q_0 = q_c, q_b = q_a$) yields a certain noncommutative Donaldson–Thomas partition function. We shall borrow some of Szendrői’s terminology, but not much of the machinery that he developed.

We will start by giving a rather algebraic definition for the bricks in a pyramid partition. Consider the quiver (or directed graph) P shown in Figure 3.5(a). The vertices of P are the elements of $\mathbb{Z}_2 \times \mathbb{Z}_2 = \{0, a, b, c\}$. The edges are labelled $\{v_1, w_1, v_2, w_2\}$.

Definition 3.5.1 *A word in P is the concatenation of the edge labels of some directed path in P . We may optionally associate a base to a word; the base is the starting vertex of the path.*

Note that a word based at 0 may also be based at c , but not at b or a . Any path in P is uniquely determined by its base and its word.

Definition 3.5.2 *Form the path algebra $\mathbb{C}P$ spanned by all words in P , and define the noncommutative quotient ring $A = \mathbb{C}P/I_W$, where*

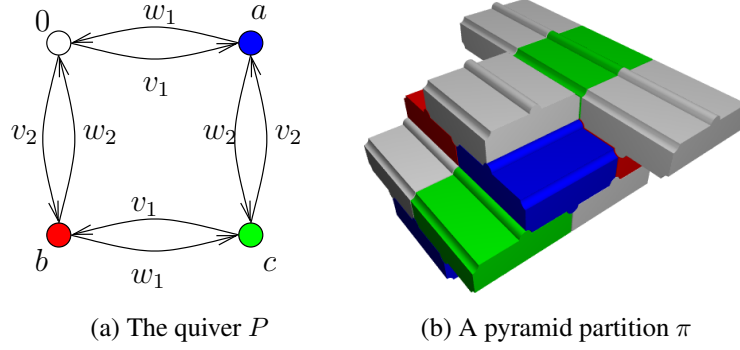
$$I_W = \langle v_1 w_i v_2 - v_2 w_i v_1, w_1 v_j w_2 - w_2 v_j w_1 \rangle, \quad i, j \in \{1, 2\}.$$

If B is a word in $\mathbb{C}P$, we write $[B]$ for its residue class in $\mathbb{C}P/I_W$.

Definition 3.5.3 *A brick is an element $[B]$ of $\mathbb{C}P/I_W$, where B is a word based at the vertex 0. Let \mathcal{B} be the set of all bricks.*

To understand how to draw Figure 3.4, we interpret the edge labels of P as vectors in \mathbb{Z}^3 .

Figure 3.5



Definition 3.5.4 *Let*

$$\begin{aligned} v_1 &= (-1, 1, 0) & v_2 &= (1, 1, 0) \\ w_1 &= (0, 1, -1) & w_2 &= (0, 1, 1). \end{aligned}$$

The position of a brick $[B]$ is the sum of the vectors corresponding to the edge labels in $[B]$. The brick corresponding to the empty walk, $[\]$, is located at the origin.

We next define a “colouring” on \mathcal{B} .

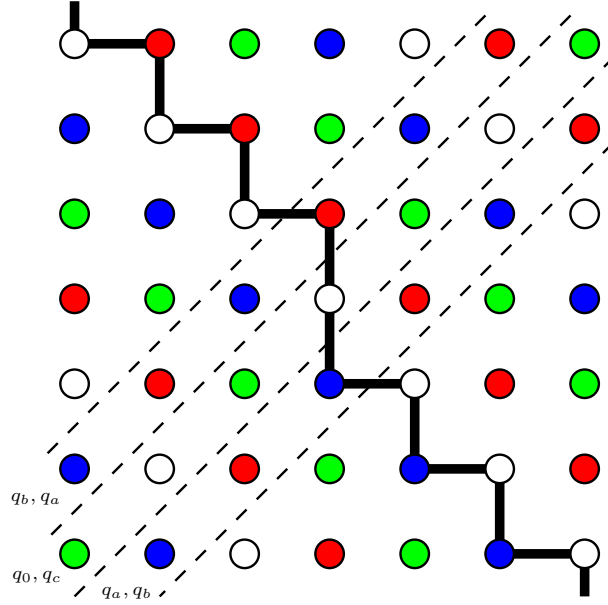
Definition 3.5.5 *Define*

$$K_{\text{pyramid}} : \mathcal{B} \longrightarrow \mathbb{Z}_2 \times \mathbb{Z}_2$$

by setting $K_{\text{pyramid}}([B])$ to be the final vertex of any path whose word is B . We call $K_{\text{pyramid}}([B])$ the colour of B .

For an example of all of these concepts, define the brick $[B]$ by the word $B = v_2 w_2 v_2 w_1$. The brick $[B]$ is based at the vertex 0 , ending at the vertex b .

Figure 3.6: A view of the pyramid \mathcal{B} from below. The bricks have been shrunk to points, and some checkerboard-coloured slices are shown.



The position of $[B]$ is $(2, 4, 0)$; $[B]$ is the c -coloured brick in the top layer of Figure 3.5b.

Note that the colour is completely determined by the x and y coordinates of $[B]$; Figure 3.6 shows the colouring as viewed from along the z axis.

Definition 3.5.6 A pyramid partition π is a subset of \mathcal{B} such that if $[B] \in \pi$ then every prefix of B also represents a brick in π .

Note that pyramid partitions may also be defined algebraically, although it is unnecessary to do so for this paper. A pyramid partition corresponds to a *framed cyclic* $\mathbb{C}P/I_W$ -module based at 0, much in the same way that a 3D Young diagram

corresponds to a monomial ideal in $\mathbb{C}[x, y, z]$. We refer the reader to [13] for further details of this approach.

Our next goal is to show that the diagonal slices of a pyramid partition interlace with one another. This will allow us to reuse the strategy of Section 3.4 to obtain a nice product formula for Z_{pyramid} .

Definition 3.5.7 *Let π be a pyramid partition. Define the k th diagonal slice of π , written π_k , to be the set of all bricks in π whose position (x, y, z) satisfies $x - y = k$.*

Lemma 3.5.8 *Let $k \geq 0$. Then*

$$\begin{aligned}\pi_{-2k} &= \{[(v_1 w_2)^k W]\} \cap \pi, \\ \pi_{2k} &= \{[(v_2 w_1)^k W]\} \cap \pi,\end{aligned}$$

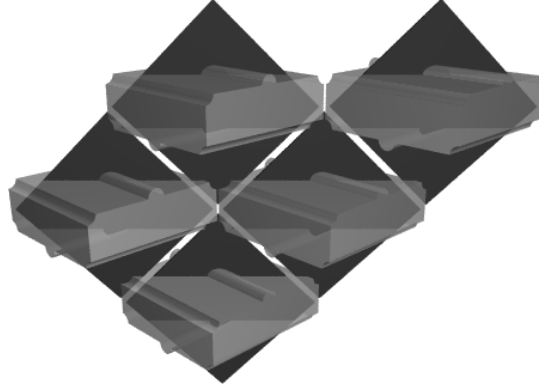
where W runs over all words in $v_1 w_1$ and $v_2 w_2$, and

$$\begin{aligned}\pi_{-2k-1} &= \{[(v_1 w_2)^k v_1 W']\} \cap \pi, \\ \pi_{2k+1} &= \{[(v_2 w_1)^k v_2 W']\} \cap \pi,\end{aligned}$$

where W' runs over all words in $w_1 v_1$ and $w_2 v_2$. Moreover, the bricks of π_k form a 2D Young diagram; the slices are single-coloured, as follows:

$$\text{Colour of } \pi_k = \begin{cases} 0 & \text{if } k \equiv 0 \pmod{4} \\ b & \text{if } k \equiv 1 \pmod{4} \\ c & \text{if } k \equiv 2 \pmod{4} \\ a & \text{if } k \equiv 3 \pmod{4}. \end{cases}$$

Figure 3.7: A diagonal slice of a pyramid partition, interpreted as a 2D Young diagram



Proof. Let us prove the first equation; the other three are similar. Note that the brick represented by the word $(v_1 w_2)^k$ is in position $(-k, 2k, k)$ and thus lies in the $-2k$ th diagonal. Appending $v_1 w_1$ or $v_2 w_2$ to this word adds $(-1, 2, -1)$ or $(1, 2, 1)$ to the position, which does not alter $x - y$.

To see that the bricks of π_{-2k} form a 2D Young diagram, observe that $w_1 v_1$ and $w_2 v_2$ commute in $\mathbb{C}P/I_w$. The suffix $(w_1 v_1)^i (w_2 v_2)^j$ corresponds to the (i, j) box in the Young diagram. Again, the other cases are similar. The colours are easy to check directly. \square

Figure 3.7 shows the central slice π_0 of the pyramid partition of Figure 3.5b. Every brick has been replaced with a square tile to make the orientation of the 2D Young diagram clear.

Lemma 3.5.9 *For $k \geq 0$, we have the following interlacing properties (where the*

prime denotes transposition of 2D Young diagrams):

$$\begin{aligned} \pi_{2k} &\succ \pi_{2k+1} & \pi'_{-2k} &\succ \pi'_{-2k-1} \\ \pi'_{2k+1} &\succ \pi'_{2k+2} & \pi_{-2k-1} &\succ \pi_{-2k-2} \end{aligned}$$

Proof. Let us handle the first case. Let R_k^j be the set of bricks in the j th column of π_k , and suppose that $|R_k^j| = \ell_k^j$. Explicitly,

$$\begin{aligned} R_{2k+1}^j &= \{(v_2 w_1)^k v_2 (w_1 v_1)^j (w_2 v_2)^i \mid 0 \leq i < \ell_{2k+1}^j\} \\ &= \{(v_2 w_1)^k (v_1 w_1)^j (v_2 w_2)^i v_2 \mid 0 \leq i < \ell_{2k+1}^j\}, \\ R_{2k}^j &= \{(v_2 w_1)^k (v_1 w_1)^j (v_2 w_2)^i \mid 0 \leq i < \ell_{2k}^j\}. \end{aligned}$$

In particular, each of the bricks in $R_{2j}^j \cup R_{2j+1}^j$ may be represented as some prefix of the word

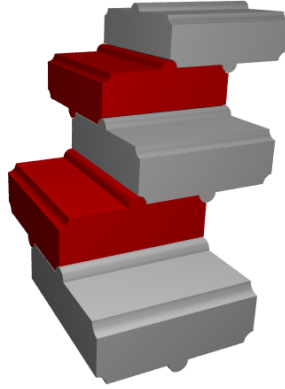
$$(v_2 w_1)^k (v_1 w_1)^j (v_2 w_2)^{\max\{\ell_{2k}^j, \ell_{2k+1}^j\}}.$$

Informally speaking, R_{2k}^j and R_{2k+1}^j form a chain of bricks, each of which rests on the previous one (see Figure 3.8). It follows from Definition 3.5.6 that $\ell_{2k}^j - \ell_{2k+1}^j \in \{0, 1\}$; then part (3) of Lemma 3.3.2 says that $\pi_{2k} \succ \pi_{2k+1}$.

Next let us see that $\pi'_{2k+1} \succ \pi'_{2k+2}$. Let $R_{i,k}$ be the i th row of π_k , with $|R_{i,k}| = \ell_{i,k}$. We have

$$\begin{aligned} R_{i,2k+2} &= \{(v_2 w_1)^k (v_2 w_2)^i (v_1 w_1)^j \mid 0 \leq j < \ell_{i,2k+2}\} \\ &= \{(v_2 w_1)^k v_2 (w_2 v_2)^i (w_1 v_1)^j \mid 0 \leq j < \ell_{i,2k+2}\}, \\ R_{i,2k+1} &= \{(v_2 w_1)^k v_2 (w_2 v_2)^i (w_1 v_1)^j \mid 0 \leq j < \ell_{i,2k+1}\}. \end{aligned}$$

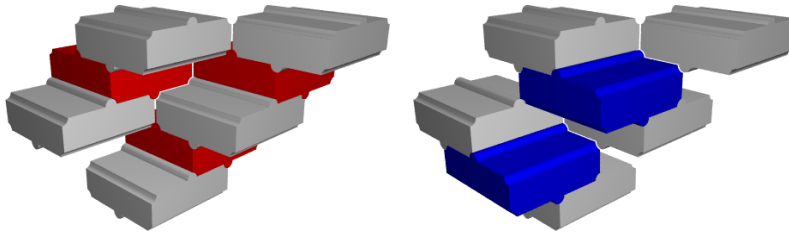
Figure 3.8: The j th columns of two adjacent slices π_0, π_1



from which it follows that $\ell_{j,2k+1} - \ell_{j,2k+2} \in \{0, 1\}$. This means that $\pi'_{2k+1} \succ \pi'_{2k+2}$. See Figure 3.9 for an illustration of the difference between the row–interlacing and column–interlacing behaviour.

The remaining cases are similar. □

Figure 3.9: Row– and column–interlacing behaviour for adjacent diagonal slices of a pyramid partition



3.6 A generating function for pyramid partitions

We will now compute the following generating function for pyramid partitions.

Definition 3.6.1 *Let π be a pyramid partition. For $g \in \mathbb{Z}_2 \times \mathbb{Z}_2$, let*

$$|\pi|_g = |K_{pyramid}^{-1}(g) \cap \pi|$$

denote the number of boxes coloured g in π . Define

$$Z_{pyramid} = \sum_{\pi \text{ pyramid partition}} \prod_{g \in \mathbb{Z}_2 \times \mathbb{Z}_2} q_g^{|\pi|_g}.$$

Theorem 3.6.2

$$Z_{pyramid} = \frac{M(1, q)^4 \widetilde{M}(q_b q_c) \widetilde{M}(q_a q_c)}{\widetilde{M}(-q_a, q) \widetilde{M}(-q_b, q) \widetilde{M}(-q_c, q) \widetilde{M}(-q_a q_b q_c, q)},$$

where $q = q_0 q_a q_b q_c$.

Theorem 3.6.2 may seem unrelated to the other theorems in this paper, but it will turn out that it is the key to computing $Z_{\mathbb{Z}_2 \times \mathbb{Z}_2}$. The proof is much like that of Theorem 3.1.4.

Proof. We define a vertex operator product which counts pyramid partitions. Let us first define an operator which sweeps out four slices of the pyramid partition at the same time. Let

$$\overline{A}'_{\pm}(x) = \Gamma_{\pm}(x) Q_b \Gamma'_{\pm}(x) Q_c \Gamma_{\pm}(x) Q_a \Gamma'_{\pm}(x) Q_0,$$

so that

$$Z_{pyramid} = \left\langle \phi \left| \cdots \overline{A}'_+(1) \overline{A}'_+(1) \overline{A}'_-(1) \overline{A}'_-(1) \cdots \right| \phi \right\rangle.$$

It is simple to check this product against Lemmas 3.5.9 and 3.5.8 to be sure that it describes the correct colouring and interlacing behaviour. Set

$$\begin{aligned} A'_+(x) &= Q_0^{-1}Q_b^{-1}Q_c^{-1}Q_a^{-1}\overline{A}'_+(x) \\ A'_-(x) &= \overline{A}'_+(x)Q_0^{-1}Q_b^{-1}Q_c^{-1}Q_a^{-1}. \end{aligned}$$

Commuting the weight operators past the vertex operators gives

$$A'_+(x) = \Gamma_+(xq_bq_cq_aq_0)\Gamma'_+(xq_cq_aq_0)\Gamma_+(xq_aq_0)\Gamma'_+(xq_0)$$

and

$$\begin{aligned} A'_-(y) &= \Gamma_-(yqq_b^{-1}q_c^{-1}q_a^{-1}q_0^{-1})\Gamma'_-(yqq_c^{-1}q_a^{-1}q_0^{-1}) \\ &\quad \cdot \Gamma_-(yqq_a^{-1}q_0^{-1})\Gamma'_-(yqq_0^{-1}) \end{aligned}$$

so that

$$Z_{\text{pyramid}} = \langle \phi | \cdots A'_+(q^2)A'_+(q)A'_+(1)A'_-(1)A'_-(q)A'_-(q^2) \cdots | \phi \rangle. \quad (3.7)$$

The commutation relation for these A' operators is

$$\begin{aligned} A'_+(x)A'_-(y) &= \frac{(1+q_bxyq)(1+q_bq_cq_axyq)(1+q_b^{-1}xyq)(1+q_cxyq)}{(1-xyq)(1-q_bq_cxyq)(1-xyq)(1-q_cq_axyq)} \\ &\quad \cdot \frac{(1+q_c^{-1}xyq)(1+q_axyq)(1+(q_bq_cq_a)^{-1}xyq)(1-q_a^{-1}xyq)}{(1-(q_bq_c)^{-1}xyq)(1-xyq)(1-(q_cq_a)^{-1}xyq)(1-xyq)} \\ &\quad \cdot A'_-(y)A'_+(x). \end{aligned}$$

Because of the mixed Γ and Γ' operators, some of the commutation factors now appear in the numerator. We now move the A'_+ operators in (3.7) to the left of the expression, while moving the A'_- operators to the right. As in the proof of Theorem 3.1.4, all of the A' vanish, and we are left with the commutator

$$Z_{\text{pyramid}} = \frac{M(1, q)^4 \widetilde{M}(q_bq_c, q) \widetilde{M}(q_aq_c, q)}{\widetilde{M}(-q_a, q) \widetilde{M}(-q_b, q) \widetilde{M}(-q_c, q) \widetilde{M}(-q_aq_bq_c, q)},$$

where $q = q_0 q_a q_b q_c$. \square

Note that this method gives an alternate proof of the result in [14], when we specialize $q_0 = q_c$, $q_1 = q_a = q_b$.

3.7 Counting $\mathbb{Z}_2 \times \mathbb{Z}_2$ -coloured 3D Young diagrams

We will now prove Theorem 3.1.5. Let us name the elements of $\mathbb{Z}_2 \times \mathbb{Z}_2$ $\{0, a, b, c\}$ as in the previous section, and recall the definition of $K_{\mathbb{Z}_2 \times \mathbb{Z}_2}$ from Theorem 3.1.5. Our set of indeterminates is $\mathcal{Q} = \{q_0, q_a, q_b, q_c\}$. Let $q = q_0 q_a q_b q_c$.

Before we proceed to compute this generating function, consider the k th diagonal slice $x - y = k$ of the positive octant. Note that we have

$$K_{\mathbb{Z}_2 \times \mathbb{Z}_2}(x, x + k, z) = (x - z)c + kb.$$

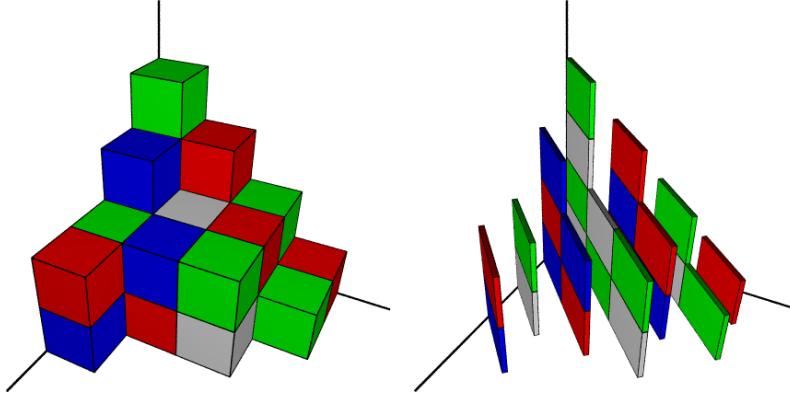
In particular, the box $(x, x + k, z)$ is coloured $k \cdot b$ if $x \equiv z \pmod{2}$, and $k \cdot b + c$ otherwise. In other words, each diagonal slice of π is now coloured in a checkerboard fashion, whereas in the \mathbb{Z}_n case, they were single-coloured (see Figure 3.10). We need to introduce a two-coloured weight function if we are to use vertex operators to compute $Z_{\mathbb{Z}_2 \times \mathbb{Z}_2}$.

Definition 3.7.1 For $g, h \in \mathbb{Z}_2 \times \mathbb{Z}_2$, let

$$Q_{gh}\lambda = q_g^{\#\{(i,j) \in \lambda \mid i \equiv j \pmod{2}\}} \cdot q_h^{\#\{(i,j) \in \lambda \mid i \not\equiv j \pmod{2}\}} \cdot \lambda.$$

We may write down a vertex operator product which sweeps out a 3D diagram in diagonal slices, according to the $\mathbb{Z}_2 \times \mathbb{Z}_2$ colouring. It is

$$\begin{aligned} Z_{\mathbb{Z}_2 \times \mathbb{Z}_2} = \langle \phi | \cdots Q_{ba} \Gamma_+(1) Q_{0c} \Gamma_+(1) Q_{ba} \Gamma_+(1) Q_{0c} \\ \cdot \Gamma_-(1) Q_{ab} \Gamma_-(1) Q_{0c} \Gamma_-(1) Q_{ab} \cdots | \phi \rangle \end{aligned} \quad (3.8)$$

Figure 3.10: Slicing a $\mathbb{Z}_2 \times \mathbb{Z}_2$ -coloured 3D diagram

Unfortunately, Γ_{\pm} no longer commutes nicely with the Q_{gh} operators, so our usual approach to computing with vertex operators fails here. The problem is fundamental, and it does not appear that we can resolve it in a natural way. We need a new idea.

However, there are two clues which tell us how to proceed. The first clue is that the desired formula for $Z_{\mathbb{Z}_2 \times \mathbb{Z}_2}$ is very close to Z_{pyramid} , so it would suffice to prove the following:

Lemma 3.7.2

$$Z_{\mathbb{Z}_2 \times \mathbb{Z}_2} = \widetilde{M}(q_a q_b, q) \cdot Z_{\text{pyramid}}.$$

The second clue is that if we attempt to compute Z_{pyramid} by slicing along lines $x + y = k$, rather than $x - y = k$, then the slices of the pyramid partition are checkerboard-coloured as well! See Figure 3.6, which shows the colouring scheme from below. The heavy black lines represent two edges of the pyramid, corresponding to prefixes of the words $(w_1 v_1)^k$ and $(w_2 v_2)^k$, so bricks which lie

on these lines represent the corners of the slices.

So, using our checkerboard coloured weight operators, we can write down a different vertex operator product which still counts pyramid partitions.

Lemma 3.7.3

$$Z_{pyramid} = \langle \phi | \cdots Q_{ba} \Gamma'_+(1) Q_{0c} \Gamma_+(1) Q_{ba} \Gamma'_+(1) Q_{0c} \\ \cdot \Gamma_-(1) Q_{ab} \Gamma'_-(1) Q_{0c} \Gamma_-(1) Q_{ab} \cdots | \phi \rangle$$

Proof. One must check that the interlacing behaviour of the slices is correct, and that the correct weights are assigned to each slice. This is similar to the proofs of Lemmas 3.5.8 and 3.5.9. \square

Observe that (3.8) is very similar to the product in Lemma 3.7.3, so we shall look for a way to transform $\Gamma_{\pm}(x)$ into $\Gamma'_{\pm}(x)$.

Definition 3.7.4 *Define*

$$E_{\pm}(x) = \exp \sum_{k \geq 1} \frac{x^{2k}}{k} \alpha_{\pm 2k}.$$

Lemma 3.7.5 *The operators E_{\pm} have the following properties:*

$$\begin{aligned} \Gamma_{\pm}(x) &= \Gamma'_{\pm}(x) E_{\pm}(x). \\ [E_{\pm}, \Gamma_{\pm}] &= 0. \\ E_+(x) \Gamma_-(y) &= \frac{1}{1 - (xy)^2} \Gamma_-(y) E_+(x). \\ \Gamma_+(x) E_-(y) &= \frac{1}{1 - (xy)^2} E_-(y) \Gamma_+(x). \\ \Gamma'_+(x) E_-(y) &= (1 - (xy)^2) E_-(y) \Gamma'_+(x). \end{aligned}$$

Proof. These are all simple applications of Corollaries 3.2.4 and 3.2.3 as well as (3.3) and (3.5). \square

In fact, unlike $\Gamma_{\pm}(x)$, $E_{\pm}(x)$ also commutes nicely with the checkerboard weight operators Q_{gh} .

Lemma 3.7.6

$$\begin{aligned} E_{-}(x)Q_{gh} &= Q_{gh}E_{-}(x\sqrt{q_gq_h}); \\ Q_{gh}E_{+}(x) &= E_{+}(x\sqrt{q_gq_h})Q_{gh}. \end{aligned}$$

Proof. The operator α_{2n} has the effect of adding all possible border strips R of length $2n$ to the boundary of a 2D Young diagram. Since the length of the strips R is even, any such R has the same Q_{gh} -weight. Indeed,

$$Q_{gh} \cdot R = (q_gq_h)^n \cdot R = (\sqrt{q_gq_h})^{|R|} \cdot R,$$

It follows that

$$\left(\sum_n \frac{x^{2n}}{n} \alpha_{-2n} \right) Q_{gh} \cdot \lambda = Q_{gh} \left(\sum_n \frac{(q\sqrt{q_gq_h})^{2n}}{n} \alpha_{-2n} \right) \cdot \lambda$$

and thus

$$E_{-}(x)Q_{gh} = Q_{gh}E_{-}(x\sqrt{q_gq_h}).$$

The case of E_{+} is similar. □

Finally, we have the following property of E_{\pm} , inherited from the corresponding property of $\alpha_{\pm n}$:

$$\begin{aligned} \langle \phi | E_{-}(x) &= \langle \phi | \\ E_{+}(x) | \phi \rangle &= | \phi \rangle \end{aligned}$$

Proof of Lemma 3.7.2. Let us alter the first line of (3.8) by transforming half of the $\Gamma_+(1)$ operators into $\Gamma'_+(1)$ operators,

$$\begin{aligned} & \left\langle \phi \left| \prod_{i=1}^{\infty} \Gamma_+(1) Q_{ba} \Gamma_+(1) Q_{0c} \right| \right\rangle \\ &= \left\langle \phi \left| \prod_{i=1}^{\infty} \Gamma_+(1) Q_{ba} \Gamma'_+(1) E_+(1) Q_{0c} \right| \right\rangle \\ &= \left\langle \phi \left| \prod_{i=1}^{\infty} \Gamma_+(1) Q_{ba} \Gamma'_+(1) Q_{0c} \right| \cdot \left| \prod_{i=0}^{\infty} E_+(q^i) E_+(Q^i \sqrt{q_b q_a}) \right| \right\rangle. \end{aligned}$$

Now, continue to move the E_+ term to the right through the second line of (3.8).

We have

$$\begin{aligned} & \left| \prod_{i=0}^{\infty} E_+(q^i) E_+(Q^i \sqrt{q_b q_a}) \right| \cdot \left| \prod_{i=1}^{\infty} \Gamma_-(1) Q_{ab} \Gamma_-(1) Q_{0c} \right| \phi \rangle \\ &= C \cdot \left| \prod_{i=1}^{\infty} \Gamma_-(1) Q_{ab} \Gamma_-(1) Q_{0c} \right| \cdot \left| \prod_{i=0}^{\infty} E_+(q^i) E_+(Q^i \sqrt{q_b q_a}) \right| \phi \rangle \\ &= C \cdot \left| \prod_{i=1}^{\infty} \Gamma_-(1) Q_{ab} \Gamma_-(1) Q_{0c} \right| \phi \rangle, \end{aligned}$$

where $C = M(1, q) M(q_b^{-1} q_c^{-1}, q)$ is the product of the commutators generated by Lemma 3.7.5. Next, change half of the Γ_- to Γ'_- in the above expression,

$$\left| \prod_{i=1}^{\infty} \Gamma_-(1) Q_{ab} \Gamma'_-(1) E_-(1) Q_{0c} \right| \phi \rangle$$

and commute them out to the left. This time, we pick up the multiplicative factor

$$\frac{M(q_a q_b, q)}{M(1, q)},$$

and the factors $M(1, q)$ cancel. We have shown that

$$Z_{\mathbb{Z}_2 \times \mathbb{Z}_2} = Z_{\text{pyramid}} \cdot \widetilde{M}(q_a q_b).$$

so Lemma 3.7.2 and Theorem 3.1.5 are now proven. \square

3.8 Future work

It would obviously be wonderful to have a combinatorial proof of these identities; such a proof might be analagous to the “ n -quotient” on 2D Young diagrams, which decomposes a Young diagram into n smaller Young diagrams and an n -core. The authors suspect, however, that such a proof would be rather difficult to find. One indication of this is that there are formulae for 3D Young tableaux which fit inside an $A \times B \times C$ box, but computational evidence suggests that there is no such nice formula for $\mathbb{Z}_2 \times \mathbb{Z}_2$ -coloured partitions.

One could attempt to compute the Donaldson–Thomas partition functions of arbitrary toric Calabi-Yau orbifolds. To this aim, it should be possible to develop an orbifold version of the topological vertex formalism following [7]; this is a work in progress. It would also be interesting to try to extend Szendrői’s work [13] in noncommutative Donaldson–Thomas theory using the results of this paper.

One box counting problem which is of great interest is to take $G = \mathbb{Z}_3$ and the colouring K given by

$$K(1, 0, 0) = K(0, 1, 0) = K(0, 0, 1) = 1.$$

However, this problem appears to be rather difficult. The group representation does not naturally embed into $SO(3)$ or $SU(2)$, so Donaldson–Thomas theory does not generate any conjectures as to what the answer might look like. Indeed, Kenyon [5] conjectures that there is no nice product formula in this example.

One unifying theme between 3D diagrams and pyramid partitions is quivers: both objects arise from a quiver path algebra modulo an ideal generated by a

superpotential [13]. Perhaps one can extend the methods to other quivers and superpotentials.

However, the most intriguing direction for future work is simply to try to understand these proofs more fully. The reader may perhaps have noticed that the appearance of pyramid partitions seems somewhat unmotivated. Undoubtedly, there is some underlying geometric or representation-theoretic reason why these product formulae exist.

Bibliography

- [1] George G. Andrews and Peter Paule, *MacMahon's dream*, Preprint, <http://www.math.psu.edu/andrews/preprints.html>.
- [2] David M. Bressoud, *Proofs and confirmations: the story of the alternating sign matrix conjecture*, Cambridge University Press, Cambridge, 1999.
- [3] William Fulton and Joe Harris, *Representation theory: A first course*, Springer-Verlag New York, Inc., 175 Fifth Ave., New York NY, 10010, USA, 1991.
- [4] Emden R. Gansner, *The enumeration of plane partitions via the Burge correspondence*, Illinois J. Math **25** (1981), no. 2, 533–554.
- [5] Richard Kenyon, Talk at the workshop on random partitions and Calabi-Yau crystals, Amsterdam, 2005. Available at <http://www.math.brown.edu/~rkenyon/talks/pyramids.pdf>.
- [6] Percy A. MacMahon, *Combinatory analysis*, Cambridge University Press, The Edinburgh Building, Cambridge, UK, 1915-16.
- [7] D. Maulik, N. Nekrasov, A. Okounkov, and R. Pandharipande, *Gromov-Witten Theory and Donaldson-Thomas Theory*, Compos. Math **142** (2006), no. 5, 1263–1304.
- [8] Andrei Okounkov, *Infinite wedge and random partitions*, Selecta Math. (N.S.) **7** (2001), no. 1, 57–81.

- [9] Andrei Okounkov and Nikolai Reshetikhin, *Correlation function of Schur process with application to local geometry of a random 3-dimensional Young diagram*, J. Amer. Math. Soc. **16** (2003), no. 3, 581–603.
- [10] ———, *Random skew plane partitions and the pearcey process*, Communications in Mathematical Physics **269** (2007), no. 3, 571–609.
- [11] Andrei Okounkov, Nikolai Reshetikhin, and Cumrun Vafa, *Quantum Calabi-Yau and classical crystals*, Progress in Mathematics **244** (2006), 597–618.
- [12] Richard P. Stanley, *Enumerative combinatorics*, vol. 2, Cambridge University Press, The Edinburgh Building, Cambridge, UK, 2001.
- [13] Balázs Szendrői, *Non-commutative Donaldson-Thomas theory and the conifold*, To appear in Geometry and Topology. arXiv:0705.3419v1 [math.AG].
- [14] Benjamin J. Young, *Computing a pyramid partition generating function with dimer shuffling*, Preprint: arXiv:0709.3079.

Chapter 4

Conclusion

4.1 Directions for future research

In addition to the future work mentioned at the end of Chapters 2 and 3, it is worth mentioning that this thesis has raised several obvious links between pyramid partitions and 3D Young diagrams. In Chapter 2, pyramid partitions are transformed into a certain type of 3D Young diagram by dimer shuffling. In Chapter 3, we define an operator which sweeps out 3D Young diagrams, and then modify it in such a way that it sweeps out pyramid partitions. These techniques are superficially unrelated to one another, but the fact that they both preserve the intricate colour schemes of the corresponding objects is unlikely to be a coincidence. It would certainly be interesting to develop some framework which genuinely explains why these techniques work, and how to generalize them.

The dimer theoretic techniques and vertex operator techniques have both been used with great success in various probabilistic questions. One can define a probability measure on the set of 3D Young diagrams, and then use vertex operator techniques to study properties of randomly chosen 3D Young diagrams [1], for example their correlation functions or limiting shape. The author intends to explore probabilistic applications of this work in future research.

4.2 Relevance of the research

The most direct application of this work is to Donaldson–Thomas theory, which is the field of mathematics which gave rise to the questions answered in this thesis. We have, implicitly, given a concrete way to calculate various types of Donaldson–Thomas invariants for the conifold [2] and for several orbifolds; hopefully, this and future work will help geometers better understand the structure of these spaces.

The work may also be of interest to those studying other aspects of 3D Young diagrams; one can now attempt (for example) to count colored 3D Young diagrams which possess various symmetries.

Finally, the dimer and vertex operator techniques are very general, and they can be used for different purposes than ours. We suspect that it will be fairly fruitful to use vertex operators to study statistical mechanical problems on the square lattice.

4.3 Strengths and weaknesses of the research

The primary strength of this work is that it has proven several concrete, enumerative formulae which answer several open questions in Donaldson–Thomas theory. The combinatorial difficulties were nontrivial and several insights were required before any progress could be made, especially in the case of the $\mathbb{Z}_2 \times \mathbb{Z}_2$ -colouring on pyramid partitions.

The primary weakness of the results is their *ad hoc* nature: the methods are rather specific to the problem at hand, which somewhat limits the scope of our work. For example, there are no other known colourings of 3D Young diagrams to which the methods of Chapter 3 immediately apply. Farther-ranging applications of these ideas will require new ideas and techniques.

Bibliography

- [1] Andrei Okounkov and Nikolai Reshetikhin. Correlation function of Schur process with application to local geometry of a random 3-dimensional Young diagram. *J. Amer. Math. Soc.*, 16(3):581–603, 2003.
- [2] Balázs Szendrői. Non-commutative Donaldson-Thomas theory and the conifold. To appear in *Geometry and Topology*. arXiv:0705.3419v1 [math.AG].

Appendix A

**Donaldson-Thomas theory of \mathbb{C}^3/G
and its crepant resolution (by Dr.
Jim Bryan)**

A.1 Review of Donaldson-Thomas theory

Donaldson-Thomas theory, in its incarnation due to Maulik, Okounkov, Nekrasov, and Pandharipande, constructs subtle integer valued deformation invariants of a threefold X out of the Hilbert scheme of subschemes of X . If X is a Calabi-Yau threefold, i.e., K_X is trivial, then this invariant has a simple formulation due to Behrend. It is given by the weighted topological Euler characteristic of the Hilbert scheme where the weighting is by ν , an integer valued constructible function which is canonically associated to any scheme [1].

Let X be a (not necessarily compact) threefold with trivial canonical class. Let $I_n(X, \beta)$ be the Hilbert scheme of subschemes $Z \subset X$ having proper support of dimension less than or equal to one and with $[Z] = \beta \in H_2(X)$ and $n = \chi(\mathcal{O}_Z)$. We define the Donaldson-Thomas invariant $N_\beta^n(X)$ to be

$$\begin{aligned} N_\beta^n(X) &= e(I_n(X, \beta), \nu) \\ &= \sum_{n \in \mathbb{Z}} e((\nu)^{-1}(n)), \end{aligned}$$

where $e(\cdot)$ denotes topological Euler characteristic and ν is Behrend's constructible function.

The invariants are assembled into the partition function Z_X^{DT} as follows. Let C_1, \dots, C_l be a basis for $H_2(X, \mathbb{Z})$ such that any effective curve class β is given by $d_1 C_1 + \dots + d_l C_l$ with $d_i \geq 0$. Let v_1, \dots, v_l be corresponding variables and let $v^\beta = v_1^{d_1} \dots v_l^{d_l}$. The Donaldson-Thomas partition function of X is defined by

$$Z_X^{DT}(v, q) = \sum_{\beta \in H_2(X, \mathbb{Z})} \sum_{n \in \mathbb{Z}} N_\beta^n(X) v^\beta q^n.$$

Define the reduced partition function by

$$\begin{aligned} Z_X^{DT}(v, q)' &= \frac{Z_X^{DT}(v, q)}{Z_X^{DT}(0, q)} \\ &= M(1, q)^{-e(X)} Z_X^{DT}(v, q) \end{aligned}$$

where the second equality is a theorem proved by [2, 12, 13].

Maulik, Nekrasov, Okounkov, and Pandharipande conjecture that Donaldson-Thomas theory is equivalent to Gromov-Witten theory. We assemble $GW_\beta^g(X)$, the genus g Gromov-Witten invariants of non-zero degree β into the reduced Gromov-Witten partition function as follows:

$$Z_X^{GW}(v, \lambda)' = \exp \left(\sum_{\beta \neq 0} \sum_{g=0}^{\infty} GW_\beta^g(X) v^\beta \lambda^{2g-2} \right).$$

Conjecture A.1.1 [14] *Under the change of variables $q = -e^{i\lambda}$ the reduced partition functions of Donaldson-Thomas and Gromov-Witten theory are equal:*

$$Z_X^{DT}(v, q)' = Z_X^{GW}(v, \lambda)'.$$

This conjecture has been proven in the case where X is a toric local surface [14] and when X is a local curve [8, 16].

A.2 Orbifold Donaldson-Thomas theory of $[\mathbb{C}^3/G]$

Extending Donaldson-Thomas theory to the case of three dimensional orbifolds is expected to be routine since the Hilbert scheme of substacks of a Deligne-Mumford stack has been constructed by Olsson and Starr [17], although it isn't clear how best to choose the discrete data in general.

The orbifolds that we consider are simple enough that we can identify the Hilbert scheme directly. Let G be a finite subgroup of $SU(3)$. A substack of $[\mathbb{C}^3/G]$ may be regarded as a G -invariant subscheme of \mathbb{C}^3 , and consequently we can regard the Hilbert scheme of $[\mathbb{C}^3/G]$ as a subset of the Hilbert scheme of \mathbb{C}^3 . Since we require our substacks to have proper support, we need only consider zero dimensional subschemes of \mathbb{C}^3 . For any G -representation R of dimension d we identify $\text{Hilb}^R([\mathbb{C}^3/G]) \subset \text{Hilb}^d(\mathbb{C}^3)$ as follows:

$$\text{Hilb}^R([\mathbb{C}^3/G]) = \{Z \subset \mathbb{C}^3 : Z \text{ is } G\text{-invariant with } H^0(\mathcal{O}_Z) = R\}.$$

This Hilbert scheme has a symmetric perfect obstruction theory induced by the G -invariant part of the perfect obstruction theory on $\text{Hilb}^d(\mathbb{C}^3) = I_d(\mathbb{C}^3, 0)$. However, we do not need this construction since we can define the Donaldson-Thomas invariants directly using Behrend's constructible function.

Definition A.2.1 *The Donaldson-Thomas invariants of $[\mathbb{C}^3/G]$ are indexed by representations of G and are given by the Euler characteristics of the Hilbert schemes, weighted by Behrend's ν function:*

$$N^R(\mathbb{C}^3/G) = e(\text{Hilb}^R([\mathbb{C}^3/G]), \nu).$$

Let q_0, \dots, q_r be variables corresponding to R_0, \dots, R_r , the irreducible representations of G . For a representation $R = d_0 R_0 + \dots + d_r R_r$, let q^R denote $q_0^{d_0} \dots q_r^{d_r}$. We define the orbifold Donaldson-Thomas partition function by

$$Z_{\mathbb{C}^3/G}^{DT}(q_0, \dots, q_l) = \sum_R N^R(\mathbb{C}^3/G) q^R$$

where R runs over all representations of G .

We now restrict our attention to groups G which are subgroups of $SO(3) \subset SU(3)$ and are Abelian. Finite subgroups of $SO(3)$ admit an ADE classification. They are the cyclic groups, the dihedral groups, and the platonic groups. The only Abelian groups from this list are the cyclic groups \mathbb{Z}_n and the Klein 4-group $\mathbb{Z}_2 \times \mathbb{Z}_2$. The action of $k \in \mathbb{Z}_n$ on \mathbb{C}^3 is given by

$$k(x, y, z) = (\omega^k x, \omega^{-k} y, z)$$

where $\omega = \exp\left(\frac{2\pi i}{n}\right)$. The action of $\mathbb{Z}_2 \times \mathbb{Z}_2 = \{0, a, b, c\}$ on \mathbb{C}^3 is given by

$$a(x, y, z) = (x, -y, -z),$$

$$b(x, y, z) = (-x, y, -z),$$

$$c(x, y, z) = (-x, -y, z).$$

As in the introduction, we choose an isomorphism ψ of the group of representations \widehat{G} with G . Explicitly, we identify $1 \in \mathbb{Z}_n$ with L , the representation of \mathbb{Z}_n where $1 \in \mathbb{Z}_n$ acts by multiplication by $\exp\left(\frac{2\pi i}{n}\right)$. For $\mathbb{Z}_2 \times \mathbb{Z}_2 = \{0, a, b, c\}$ we identify a, b , and c with the representations α, β , and γ given by the action on the x, y , and z coordinates of \mathbb{C}^3 respectively.

Theorem A.2.2 *Let q_k be the variable corresponding to the group element $k \in \mathbb{Z}_n$ and the character L^k . Then*

$$Z_{\mathbb{C}^3/\mathbb{Z}_n}^{DT}(q_0, \dots, q_{n-1}) = Z_{\mathbb{Z}_n}(-q_0, q_1, \dots, q_{n-1})$$

where $Z_{\mathbb{Z}_n}$ is the \mathbb{Z}_n -colored 3D diagram partition function introduced and computed in the main body of the paper (Theorem 3.1.4).

Let $\{q_0, q_a, q_b, q_c\}$ be variables corresponding to $\{0, a, b, c\}$, the group elements of $\mathbb{Z}_2 \times \mathbb{Z}_2$, and $\{1, \alpha, \beta, \gamma\}$, the characters of $\mathbb{Z}_2 \times \mathbb{Z}_2$. Then

$$Z_{\mathbb{C}^3/\mathbb{Z}_2 \times \mathbb{Z}_2}^{DT}(q_0, q_a, q_b, q_c) = Z_{\mathbb{Z}_2 \times \mathbb{Z}_2}(q_0, -q_a, -q_b, -q_c)$$

where $Z_{\mathbb{Z}_2 \times \mathbb{Z}_2}$ is the $\mathbb{Z}_2 \times \mathbb{Z}_2$ -colored 3D diagram partition function introduced and computed in the main body of the paper (Theorem 3.1.5).

PROOF: Let G be \mathbb{Z}_n or $\mathbb{Z}_2 \times \mathbb{Z}_2$ and let $T \subset (\mathbb{C}^\times)^3$ be the subtorus with $t_1 t_2 t_3 = 1$. The action of T on \mathbb{C}^3 commutes with the action of G and hence defines a T -action on $[\mathbb{C}^3/G]$ and on $\text{Hilb}^R(\mathbb{C}^3/G)$. The fixed points of T in $\text{Hilb}^R(\mathbb{C}^3/G) \subset \text{Hilb}^{\dim R}(\mathbb{C}^3)$ are isolated, even infinitesimally [2, Lemma 4.1], and they correspond to monomial ideals in $\mathbb{C}[x, y, z]$. The monomial ideals in turn correspond to 3D Young diagrams π where if Z denotes the T -fixed subscheme of \mathbb{C}^3 , then

$$H^0(\mathcal{O}_Z) = \sum_{(i,j,k) \in \pi} t_1^i t_2^j t_3^k$$

as a T -representation viewed as a polynomial in t_1, t_2, t_3 modulo the relation $t_1 t_2 t_3 = 1$. Following [14], we adopt the notation

$$Q_\pi = \sum_{(i,j,k) \in \pi} t_1^i t_2^j t_3^k.$$

By [2, Prop. 3.3], the ν -weighted Euler characteristic of $\text{Hilb}^R(\mathbb{C}^3/G)$ is given by a sum over the T -fixed points, counted with sign given by the parity of the dimension of the Zariski tangent space of $\text{Hilb}^R(\mathbb{C}^3/G)$ at a fixed point corresponding to 3D diagram π . Hence both the Donaldson-Thomas and the diagram partition functions are given by a sum over 3D diagrams, weighted, up to a sign, by the same variables. Thus our main task is to determine the sign.

Let π be a 3D diagram having $N = |\pi|$ boxes and having $|\pi|_g$ boxes of color $g \in G$. Let T_π denote the Zariski tangent space of $\text{Hilb}^N(\mathbb{C}^3)$ at the subscheme corresponding to π . Let

$$(T_\pi)^0 \subset T_\pi$$

be the Zariski tangent space of $\text{Hilb}^R([\mathbb{C}^3/G]) \subset \text{Hilb}^N(\mathbb{C}^3)$ at the same point. T_π can be regarded as both a T -representation and a G -representation. $(T_\pi)^0$ is given by the G -invariant subspace of T_π .

The difference of T_π and its dual T_π^\vee , regarded as a virtual $(\mathbb{C}^\times)^3$ -representation, is computed in [14, equation (13)] and given by

$$T_\pi - T_\pi^\vee = Q_\pi - \frac{\overline{Q}_\pi}{t_1 t_2 t_3} + Q_\pi \overline{Q}_\pi \frac{(1-t_1)(1-t_2)(1-t_3)}{t_1 t_2 t_3}$$

where

$$\overline{Q}_\pi(t_1, t_2, t_3) = Q_\pi(t_1^{-1}, t_2^{-1}, t_3^{-1}).$$

Using the relation $t_1 t_2 t_3 = 1$ to eliminate t_3 from the above expression, we can regard $T_\pi - T_\pi^\vee$ as an element in

$$R(T) \cong \mathbb{Z}[t_1, t_2, t_1^{-1}, t_2^{-1}],$$

the virtual representation ring of T .

Following [14], we let

$$V_\pi = Q_\pi + Q_\pi \overline{Q}_\pi (1-t_1)(1-t_2)t_1^{-1}t_2^{-1}$$

which satisfies the easily verified equation

$$T_\pi - T_\pi^\vee = V_\pi - V_\pi^\vee \tag{A.1}$$

in $R(T)$, and also has the crucial property that the constant term of V_π is even [14, Lemma 10]. These facts allow us to use V_π as a surrogate for T_π when computing the parity of the dimension:

Lemma A.2.3 *Let $(T_\pi)^0$ and $(V_\pi)^0$ denote the G -invariant part of T_π and V_π respectively, then*

$$\dim (T_\pi)^0 \equiv \text{vdim} (V_\pi)^0 \pmod{2}.$$

PROOF: From equation (A.1) we see that $T_\pi - V_\pi$ is self-dual. Thus all non-constant monomials occur in pairs of the form $a_{ij}(t_1^i t_2^j + t_1^{-i} t_2^{-j})$. Moreover, the constant term of V_π is even [14, Lemma 10] and the constant term of T_π is zero [2, Lemma 4.1]. Thus we have

$$\text{vdim}(T_\pi - V_\pi) \equiv 0 \pmod{2}.$$

Indeed, the above argument shows that if we restrict $T_\pi - V_\pi$ to any self-dual collection of weights, the virtual dimension will be even. In particular, the G -invariant part of $T_\pi - V_\pi$ has even virtual dimension, which proves the lemma.

□

To compute the parity of the G -invariant part of V_π , we work in the representation ring of G with mod 2 coefficients. The restriction map

$$R(T) \cong \mathbb{Z}[t_1, t_2, t_1^{-1}, t_2^{-1}] \rightarrow R_{\mathbb{Z}_2}(G)$$

is explicitly given by

$$(t_1, t_2) \mapsto (L, L^{-1})$$

in the case where $G = \mathbb{Z}_n$, and by

$$(t_1, t_2) \mapsto (\alpha, \beta)$$

in the case where $G = \mathbb{Z}_2 \times \mathbb{Z}_2$.

For any $W \in R_{\mathbb{Z}_2}(G)$ and any irreducible representation ζ , let $[W]_\zeta \in \mathbb{Z}_2$ denote the coefficient of ζ in W . We compute $[V_\pi]_1$ in

$$R_{\mathbb{Z}_2}(\mathbb{Z}_n) = \mathbb{Z}_2[L]/(L^n - 1)$$

as follows.

$$\begin{aligned}
[V_\pi]_1 &= [Q_\pi + Q_\pi \overline{Q}_\pi (1 - L)(1 - L^{-1})]_1 \\
&= [Q_\pi]_1 + [Q_\pi \overline{Q}_\pi (L + L^{-1})]_1 \\
&= [Q_\pi]_1 + [Q_\pi \overline{Q}_\pi]_{L^{-1}} + [Q_\pi \overline{Q}_\pi]_L \\
&= [Q_\pi]_1 \\
&= |\pi|_0 \pmod{2}
\end{aligned}$$

Since $[V_\pi]_1$ is equal to the dimension of the \mathbb{Z}_n -invariant part of T_π modulo 2, the 3D diagram π is counted with sign $(-1)^{|\pi|_0}$ in the Donaldson-Thomas partition function of $\mathbb{C}^3/\mathbb{Z}_n$. This proves first part of Theorem A.2.2.

We now compute $[V_\pi]_1$ in

$$R_{\mathbb{Z}_2}(\mathbb{Z}_2 \times \mathbb{Z}_2) = \mathbb{Z}_2[\alpha, \beta]/(\alpha^2 - 1, \beta^2 - 1).$$

We use the fact that in this ring, the square of an arbitrary element is equal to the sum of its coefficients:

$$(n_1 + n_2\alpha + n_3\beta + n_4\alpha\beta)^2 = n_1 + n_2 + n_3 + n_4,$$

and we compute as follows.

$$\begin{aligned}
[V_\pi]_1 &= [Q_\pi + Q_\pi \overline{Q}_\pi (1 - \alpha)(1 - \beta)\alpha\beta]_1 \\
&= [Q_\pi]_1 + [Q_\pi^2 (1 + \alpha + \beta + \alpha\beta)]_1 \\
&= [Q_\pi]_1 + [|\pi|(1 + \alpha + \beta + \alpha\beta)]_1 \\
&= |\pi|_0 + |\pi| \pmod{2} \\
&= |\pi|_a + |\pi|_b + |\pi|_c \pmod{2}.
\end{aligned}$$

Since $[V_\pi]_1$ is equal to the dimension of the $\mathbb{Z}_2 \times \mathbb{Z}_2$ -invariant part of T_π modulo 2, the 3D diagram π is counted with sign $(-1)^{|\pi|_a+|\pi|_b+|\pi|_c}$ in the Donaldson-Thomas partition function of $\mathbb{C}^3/\mathbb{Z}_2 \times \mathbb{Z}_2$. This proves the remaining part of Theorem A.2.2 and so the proof of Theorem is complete. \square

Remark A.2.4 *For any finite Abelian subgroup $G \subset SU(3)$, the Donaldson-Thomas invariants of \mathbb{C}^3/G are given by a signed count of boxes colored by G . However, it is not always true that this sign is obtained by simply changing the signs of some of the variables. For example, consider the case of $G = \mathbb{Z}_3$ acting on \mathbb{C}^3 with equal weights on all three factors. The sign associated to a 3D partition π can be computed by the methods of this appendix and is given by*

$$(-1)^{|\pi|(1+|\pi|_0|\pi|_1|\pi|_2)+|\pi|_0}.$$

Thus the colored 3D diagram partition function and the Donaldson-Thomas partition function are not related in an obvious way.

A.3 The Donaldson-Thomas crepant resolution conjecture

A well known principle in physics asserts that string theory on a Calabi-Yau orbifold X is equivalent to string theory on any crepant resolution $Y \rightarrow X$. Consequently, it is expected that mathematical counterparts of string theory, such as Gromov-Witten theory or Donaldson-Thomas theory, should be equivalent on X

and Y . Precise formulations of these equivalences are known as crepant resolution conjectures. The crepant resolution conjecture in Gromov-Witten theory goes back to Ruan, and has recently undergone successive refinements [18, 6, 9, 10].

In this section we formulate a crepant resolution conjecture for Donaldson-Thomas theory. Our conjecture has somewhat limited scope: we stick to the “local case” where X is of the form $[\mathbb{C}^3/G]$, and (for reasons explained below) we impose the *hard Lefschetz condition* [6, Defn 1.1], which implies [5] that G is a finite subgroup of either $SU(2) \subset SU(3)$ or $SO(3) \subset SU(3)$.

The most straightforward formulation of the crepant resolution conjecture in Donaldson-Thomas theory posits that the partition functions of the orbifold and its resolution are equal after some natural change of variables. For the orbifold $[\mathbb{C}^3/G]$, we saw in the previous section that the partition function has variables naturally indexed by irreducible G -representations. By the classical McKay correspondence, the crepant resolution $Y_G \rightarrow \mathbb{C}^3/G$ given by the G -Hilbert scheme has a basis of $H_*(Y_G)$ also labelled by irreducible G -representations [4, 15]. However, the variables of the Donaldson-Thomas partition function of Y_G correspond to a basis of $H_0(Y_G) \oplus H_2(Y_G)$. So in order to get the number of variables of $Z_{Y_G}^{DT}$ and $Z_{\mathbb{C}^3/G}^{DT}$ to match, we need

$$H_*(Y_G) = H_0(Y_G) \oplus H_2(Y_G).$$

This occurs if and only if $Y_G \rightarrow \mathbb{C}^3/G$ is a semi-small resolution. This condition is equivalent to the orbifold satisfying the hard Lefschetz condition.

Conjecture A.3.1 *Let X be a local, 3 dimensional, Calabi-Yau orbifold satisfying the hard Lefschetz condition, namely, $X = X_G = [\mathbb{C}^3/G]$ where G is a finite subgroup of either $SU(2) \subset SU(3)$ or $SO(3) \subset SU(3)$.*

Let q_0, q_1, \dots, q_l be variables corresponding to the irreducible G -representations R_0, R_1, \dots, R_l where R_0 is the trivial representation. Let $Y_G \rightarrow X_G$ be the crepant resolution given by the G -Hilbert scheme and let v_1, \dots, v_l be the variables corresponding to the basis of curve classes in Y_G labelled by the non-trivial G -representations R_1, \dots, R_l .

Then the Donaldson-Thomas partition functions of Y_G and X_G are related by the formula

$$Z_{X_G}^{DT}(q_0, \dots, q_l) = M(1, q)^{-e(Y_G)} Z_{Y_G}^{DT}(q, v_1, \dots, v_l) Z_{Y_G}^{DT}(q, v_1^{-1}, \dots, v_l^{-1})$$

under the identification of the variables

$$\begin{aligned} v_i &= q_i \quad \text{for } i = 1, \dots, l, \\ q &= q^{R_{reg}} \\ &= q_0^{\dim R_0} \dots q_l^{\dim R_l}. \end{aligned}$$

Proposition A.3.2 Conjecture A.3.1 holds for G Abelian, namely for $G = \mathbb{Z}_n$ or $G = \mathbb{Z}_2 \times \mathbb{Z}_2$.

Remark A.3.3 Szendrői proved [19] that a similar relationship holds between the Donaldson-Thomas partition functions of the non-commutative conifold singularity and its small resolution.

Remark A.3.4 The Gromov-Witten partition function of Y_G has been computed for all G in $SU(2)$ or $SO(3)$ in [5] (see also Remark A.3.5). This provides, via the MNOP conjecture, a prediction for $Z_{Y_G}^{DT}$ and hence our conjecture A.3.1 gives a prediction for $Z_{\mathbb{C}^3/G}^{DT}$ which can be tested term by term. Verification of this prediction for terms of low order has been obtained by D. Steinberg in the case where G is the quaternion 8 group.

In light of Theorems 3.1.4, 3.1.5, and A.2.2, Proposition A.3.2 is equivalent to Theorem 3.1.7 which we prove here.

A.3.1 Proof of Proposition A.3.2 / Theorem 3.1.7:

Since G is Abelian, Y_G is toric and so via [14, Theorems 2 and 3], the reduced Donaldson-Thomas partition function of Y_G is equal to the reduced Gromov-Witten partition function of Y_G after the change of variables $q = -e^{i\lambda}$. Thus it suffices to compute the Gromov-Witten partition function of Y_G ¹. The pithiest way to encode the Gromov-Witten invariants is in terms of Gopakumar-Vafa invariants, or so called BPS state counts. It is well known that each genus zero BPS state count n_β^0 contributes a factor of $M(v^\beta, -e^{i\lambda})^{-n_\beta^0}$ to the Gromov-Witten partition function (see for example the proof of Theorem 3.1 in [3]). Thus the content of Theorem 3.1.7 is that $Y_{\mathbb{Z}_n}$ has genus 0 Gopakumar-Vafa invariants occurring in the classes $C_a + \dots + C_b$ for $0 < a \leq b < n$ with value -1, and that $Y_{\mathbb{Z}_2 \times \mathbb{Z}_2}$ has genus 0 Gopakumar-Vafa invariants occurring in the classes C_a, C_b, C_c , and $C_a + C_b + C_c$ with value 1 and in the classes $C_a + C_b, C_a + C_c$, and $C_b + C_c$ with value -1. Moreover, all other Gopakumar-Vafa invariants are zero. These assertions are proved in [11]: the case of $Y_{\mathbb{Z}_2 \times \mathbb{Z}_2}$ is Corollary 16 and Proposition 19 and the case

¹In [14] it is shown that the reduced Donaldson-Thomas partition function of a toric Calabi-Yau threefold can be computed via the topological vertex formalism. In general, the topological vertex formalism has been proven to compute the Gromov-Witten partition function only in the “two-leg” case. While $Y_{\mathbb{Z}_n}$ is a local surface and can be computed with two-leg vertices, $Y_{\mathbb{Z}_2 \times \mathbb{Z}_2}$ has the geometry of the closed topological vertex [7] and requires a three-leg vertex. However, in this case, the invariants have been computed by both the vertex formalism as well as by localization and have been shown to agree [11]. Thus we know that the Gromov-Witten/Donaldson-Thomas correspondence holds for both $Y_{\mathbb{Z}_n}$ and $Y_{\mathbb{Z}_2 \times \mathbb{Z}_2}$.

of $Y_{\mathbb{Z}_n}$ is Proposition 12. □

Remark A.3.5 *The Gromov-Witten and Donaldson-Thomas theories of Y_G are equivariant theories and so in general depend on the choice of the torus action. In this paper, we have assumed that the torus is chosen to act trivially on the canonical class. This choice is required to apply the topological vertex formalism as we have done in the above proof. We warn the reader that the computation of the Gromov-Witten invariants of Y_G for general $G \subset SO(3)$ done in [5] is done using the \mathbb{C}^\times action induced from the diagonal action on \mathbb{C}^3/G . This does not change which classes carry Gopakumar-Vafa invariants, but it can change the values of the invariants in those curve classes that admit deformations to infinity.*

Bibliography

- [1] K. Behrend, *Donaldson-Thomas type invariants via microlocal geometry*, ArXiv: math.AG/0507523.
- [2] K. Behrend and B. Fantechi, *Symmetric obstruction theories and Hilbert schemes of points on threefolds*, ArXiv: math.AG/0512556.
- [3] Kai Behrend and Jim Bryan, *Super-rigid Donaldson-Thomas invariants*, Mathematical Research Letters **14** (2007), no. 4, 559–571, arXiv version: math.AG/0601203.
- [4] Tom Bridgeland, Alastair King, and Miles Reid, *The McKay correspondence as an equivalence of derived categories*, J. Amer. Math. Soc. **14** (2001), no. 3, 535–554 (electronic). MR MR1824990 (2002f:14023)
- [5] Jim Bryan and Amin Gholampour, *The Quantum McKay correspondence for polyhedral singularities*, In preparation.
- [6] Jim Bryan and Tom Graber, *The crepant resolution conjecture*, To appear in *Algebraic Geometry — Seattle 2005 Proceedings*, arXiv: math.AG/0610129.
- [7] Jim Bryan and Dagan Karp, *The closed topological vertex via the Cremona transform*, Journal of Algebraic Geometry **14** (2005), 529–542, arXiv version math.AG/0311208.
- [8] Jim Bryan and Rahul Pandharipande, *The local Gromov-Witten theory of curves*, J. Amer. Math. Soc. **21** (2008), no. 1, 101–136 (electronic), With an appendix by Bryan, C. Faber, A. Okounkov and Pandharipande. MR MR2350052

- [9] Tom Coates, Alessio Corti, Hiroshi Iritani, and Hsian-Hua Tseng, *Wall-Crossings in Toric Gromov-Witten Theory I: Crepant Examples*, arXiv:math.AG/0611550.
- [10] Tom Coates and Yongbin Ruan, *Quantum Cohomology and Crepant Resolutions: A Conjecture*, arXiv:0710.5901.
- [11] Dagan Karp, Chiu-Chu Melissa Liu, and Marcos Marino, *The local Gromov-Witten invariants of configurations of rational curves*, arXiv:math.AG/0506488.
- [12] M. Levine and R. Pandharipande, *Algebraic cobordism revisited*, arXiv:math/0605196.
- [13] Jun Li, *Zero dimensional Donaldson-Thomas invariants of threefolds*, Geom. Topol. **10** (2006), 2117–2171 (electronic). MR MR2284053 (2007k:14116)
- [14] D. Maulik, N. Nekrasov, A. Okounkov, and R. Pandharipande, *Gromov-Witten theory and Donaldson-Thomas theory. I*, Compos. Math. **142** (2006), no. 5, 1263–1285. MR MR2264664 (2007i:14061)
- [15] John McKay, *Graphs, singularities, and finite groups*, The Santa Cruz Conference on Finite Groups (Univ. California, Santa Cruz, Calif., 1979), Proc. Sympos. Pure Math., vol. 37, Amer. Math. Soc., Providence, R.I., 1980, pp. 183–186. MR MR604577 (82e:20014)
- [16] A. Okounkov and R. Pandharipande, *The local Donaldson-Thomas theory of curves*, arXiv:math.AG/0512573.

- [17] Martin Olsson and Jason Starr, *Quot functors for Deligne-Mumford stacks*, Comm. Algebra **31** (2003), no. 8, 4069–4096, Special issue in honor of Steven L. Kleiman. MR MR2007396 (2004i:14002)
- [18] Yongbin Ruan, *The cohomology ring of crepant resolutions of orbifolds*, Gromov-Witten theory of spin curves and orbifolds, Contemp. Math., vol. 403, Amer. Math. Soc., Providence, RI, 2006, pp. 117–126. MR MR2234886
- [19] Balázs Szendrői, *Non-commutative Donaldson-Thomas theory and the conifold*, To appear in Geometry and Topology. arXiv:0705.3419v1 [math.AG].